

Trades Fragmentation and Volatility of Volatility Dynamics: a network analysis

Abstract

We assess the relationship between trades fragmentation in equity markets, and the structure of volatility networks inspired from the volatility-of-volatility (VoV) approach. Volatility networks are an original method of measurement and visualization of the common component of volatilities. In particular, we use the topological distance and connectivity indicators describing the structure of these networks as alternative proxies of the VoV. We apply threshold effects regression models on French equity market data after the introduction of MIFID, both at the portfolio level and at the asset level with panel tests. We show that market fragmentation has a nonlinear impact on all VoV proxies. In particular, network distances are reduced, and connectivity is enhanced, suggesting a reduction in the VoV caused by both a contraction of volatility networks and a change in their structure. These effects are both nonlinear with multiple regimes as fragmentation increases and then stabilizes, and heterogeneous as fragmentation at the asset level diverges over time. They are robust to tests at the portfolio and individual asset levels. These original findings are of interest to market operators, regulators, and public authorities.

JEL classification: C65, G12, G14, G18.

Keywords: Financial networks, market microstructure, volatility-of-volatility, threshold models, MiFID, RegNMS, trades fragmentation.

1 Introduction

Trades in equity securities are said to be fragmented when securities are not solely traded in the market, which first listed them, but also in other stock exchanges or trading platforms. This competition between stock exchanges aims to improve efficiency and increase market liquidity. However, after the major regulatory shocks enhancing competition in the United States (Regulation National Market System, Reg NMS) in October 2006; and introducing it in Europe (Markets in Financial Instruments Directive, MiFID) in November 2007, volatility sharply increases. The Global financial crisis may not be the sole cause, given the magnitude of these regulatory shocks. As of January 2022, there are more than 40 different venues in European equity markets. In the United States, NYSE and NASDAQ order book trades account for no more than 40% of the notional value of overall trades (CBOE, 2022b).

The issue of trades fragmentation has always been discussed in terms of market microstructure. In the groundbreaking article of Hamilton (1979), in the absence of monopoly, the favorable competition effect would predominate over the inefficiency resulting from the impossibility of reducing costs through economies of scale. In the recent literature, Foucault and Menkveld (2008), in the case of the Dutch stock market; Chlistalla and Lutat (2011), in the case of the French stock market; or He et al. (2015), in the case of 16 stock markets involving Chi-X before its merger with BATS, support the hypothesis of a predominant favorable competition effect. By contrast, Goldstein et al. (2008), in the case of NASDAQ securities, find particularly contrasting effects, especially for the less liquid securities. Baldauf and Mollner (2021), in the case of the Australian stock market, do not find evidence of a favorable effect of fragmentation; and Cimon (2021) shows in a theoretical model that the benefits of competition may be limited by conflicts of interest between brokers, who choose the venue on the basis of fees, and investors, whose utility also depends on the quality of execution. In addition, fragmentation between lit and dark markets also affects liquidity and price formation (Gresse, 2017).

In the context of a large prevalence of high frequency trading, a reciprocal relationship between liquidity and price formation may be observed in fragmented markets, particularly in the case of large capitalizations, held by financial institutions (Zhang, 2010). Various aspects of price formation can be affected, including the impact of incoming orders and the subsequent price changes (i.e. price impact, Chen and Duffie, 2020), or the ability of some traders to manipulate prices (Easley et al., 1996). In particular, sending large non-marketable orders affects the efficiency of price formation. These trades are in the opposite direction to permanent price changes and in the same direction as transitory pricing errors (Brogaard et al., 2014). They are also strongly correlated, which creates the conditions for self-fulfilling dynamics (Chaboud et al., 2014). In general, the effect of trades fragmentation on price formation is controversial, and heterogeneous depending on trade volumes.

We propose an empirical study of the relationship between equity markets fragmentation and volatility networks inspired from the volatility-of-volatility (VoV) approach,

using French equity market data after the introduction of the MiFID directive. This approach is, to the best of our knowledge, twofold original. First, the existing markets microstructure literature is focused on the relationship between fragmentation and volatility at the individual level, not on the relationship between fragmentation and the structure of volatility networks. Second, we use the structure of volatility networks as an original measure and representation of the common component of volatilities. This allows us to use the corresponding topological network indicators as VOV proxies and to discuss the results in light of the VoV approach. The principle is that the assets that have a low common component and contribute the most to the VOV are located at the periphery of the network, with low connectivity and high distances. The assets that have the highest common component and contribute the least are located in the core, with high connectivity and low distances. Since the VoV has been shown to predict stock markets returns by Bollerslev et al. (2009) and to be priced in a market-based assets pricing model by Chen et al. (2022), the question of its relationship with fragmentation is a major issue, for market operators and also public authorities and supervisors.

To capture the effect of fragmentation not on individual volatilities, but on the structure of volatility networks, in the spirit of the VOV approach, we rely on the literature on graph representations of stock markets following the groundbreaking papers of Mantegna (1999), Bonanno et al. (2001) and Tumminello et al. (2007). This literature studies, in particular, minimal spanning trees (e.g., Held and Karp, 1970) providing network representations of the common component of assets prices indicators. The structure of these networks can be described using different local and global distance and connectivity indicators, so that we could capture different forms of effects of fragmentation on the structure of volatility networks. Like ecosystems, which are also an usual application of minimal spanning trees, the structure of stock market networks changes over time. This happens especially in cases of phase transitions caused by environmental changes, when switching from one equilibrium to another (May et al., 2008; Soramäki et al., 2007).¹

To capture these shifts, our empirical modeling method combines network methods with a second field of computational economics: nonlinear financial dynamics. In order to enable our modeling to be as flexible as possible to assess for the impact of fragmentation on the structure of volatility networks, and in particular to take into account further nonlinearity caused by the regulatory environment change, we propose a threshold econometric specification. This modeling enables us to apprehend asymmetry and nonlinearity in the relationship between fragmentation and network indicators. Further, it is relevant as it also enables us to reproduce time-varying effects of fragmentation on the structure of volatility networks. Indeed, it is expected that the implementation of MiFID has been carried and integrated by investors and regulators step by step and therefore that its consequences enter also progressively.

¹For a recent survey of empirical analyses of complex networks in computational finance, see Iori and Mantegna (2018).

Besides the usual result in the recent literature on market microstructure stating that the fragmentation of trades on a given security affects its volatility, we show that fragmentation also affects the structure of French equity market volatility networks over the study period. In the first regime, immediately following the regulatory shock, the most fragmented stocks are generally at the core of the volatility network, characterized by short local and global distance measures and strong direct connectivity. In the next regimes, with the gradual stabilization of fragmentation, the distances decreasing effect of fragmentation tends to be reinforced while the effect of increasing connectivities tends to become stronger, particularly for second rank connectivities. Tests of the VoV proxies at the portfolio level show that these effects are not uniform and are mainly exerted on the most fragmented assets. In general, market fragmentation tends to make volatility networks denser, which can be interpreted as a reduction of VOV. These findings shed new light on the study of the effects of fragmentation on price formation for at least two reasons. First, the existing literature highlights individual effects that are rather favorable for the most liquid securities and less favorable for the others. Our original network measures illustrate, beyond these individual effects, the existence of aggregated effects. Second, the existence of a statistically significant relationship between market fragmentation and networks proxies of the VoV suggests that the consequences of market fragmentation on price formation may be multiple and may operate through different channels. The microstructure literature largely focuses on market makers' decisions in different regulatory and competitive environments. Our results suggest that fragmentation, by affecting the VoV, also affects equity market returns (e.g., Bollerslev et al., 2009; Chen et al., 2022), and thus has direct effects on investors' decisions.

The rest of the paper is organised as follows. Section 2 is devoted to the presentation of the methods. We discuss the main results and their implications in section 3. Section 4 concludes the paper.

2 Econometric Methodology

In this section we present we first present the network methodology and the related topological indicators (section 2.1). Then we present the econometric linear and non-linear methodology for modeling the relationship between fragmentation and the VoV, at the portfolio and individual asset levels (section 2.2).

2.1 Network Methodology and Indicators

2.1.1 Sparse Network Representations

The topological approach of equity markets consists in building networks representations, starting from time series of price indicators. The network is composed of nodes, representing assets; and edges representing the connexions between the assets. The edges are characterized by distances representing the common component of the time

series of price indicators between assets (Soramäki et al., 2007). In this sense, a network of assets produced from time series of volatilities is directly related to the contributions of these assets to the VoV. This approach constitutes a new methodological contribution to assess for the dynamics of VoV using network techniques. In particular, the assets with the highest common component of volatility (and thus the lowest contribution) are at the core of the network, connected by small distances. To the contrary, the assets with the lowest common component of volatility (and thus the highest contribution) are in peripheral positions and are connected by long distances. At the overall level, the larger the network, the stronger the individual common components and the VoV. The denser the network, the lower the individual common components and the VoV. To our knowledge, this is the first paper that proposes an analysis of VoV using a network method.

It is important to note that there are two types of financial networks in the literature: asset networks, derived from price indicators, which we apply here; and networks of financial institutions, representing trades. In the recent literature, networks of financial institutions are generally used to measure systemic risk (de Souza et al., 2016) and assess its consequences (Chinazzi et al., 2013) and those of mitigation policies (Capponi and Chen, 2015). Asset networks are complete by their nature: each pair of assets is associated with an edge. Financial institutions networks are generally not complete. However, the density of edges usually remains too high to provide meaningful representations. Thus in both cases economic analysis requires to compute sparse networks by isolating the most relevant edges.

The minimal spanning tree (Held and Karp, 1970) is the most commonly used representation for this purpose (Mantegna, 1999; Bonanno et al., 2001; Tumminello et al., 2007). For any complete or dense network, it provides a subgraph, *i.e.* a graph composed of the same nodes and a lower number of edges. The literature shows that the minimal spanning tree subgraph takes into account the most economically relevant relationships (Mantegna, 1999). Any connected network has a unique minimal spanning tree. The corresponding hierarchical tree, derived from the single linkage or nearest neighbor method, has the same branches. We use both representations, the minimal spanning tree disclosing a branching composed of groups of assets with a relatively high common component of time series; while the hierarchical tree discloses the hierarchy of distances and therefore the similarity of time series within and between groups.

2.1.2 Network methods

In the existing literature on stock market networks, the correlation matrix of time series of prices is the most commonly used as the starting point of the computation of minimal spanning trees. We use the correlation matrix of time series of volatilities, for two reasons. First, in the market microstructure literature, the assessment of the impact of trades fragmentation on price formation broadly relies on the empirical relationship between trades fragmentation and volatility (see Hamilton, 1979, but also Brogaard et al., 2010, Zhang, 2010 and Kirilenko et al., 2014). Second, as discussed earlier, the

minimal spanning trees obtained from time series of volatilities are related to the VoV. The analysis of the relationship between the fragmentation of trades and the dynamic structure of the minimum spanning trees of volatilities thus allows an approach at the most granular level of the effect of fragmentation on the VoV.

We apply a measure of volatility based on daily high, low and close (HLC) values, in the spirit of Yang and Zhang (2000), Magdon-Ismail and Atiya (2003) and Horst et al. (2012), for several reasons. First, fragmentation measures, with which we study the empirical relationship, are not available in intra-day frequency. Volatility measures with intra-day frequencies are therefore not suitable. In this context, HLC volatility has two advantages over standard deviation measures of volatility. First, it allows us to take into account the information on intra-day variations contained in the daily data, unlike indicators calculated from closing prices alone. Second, it does not require the use of sliding windows, that smooth out the peaks. This advantage is all the more important since we already use sliding windows in the last step of the network indicator calculation method.

For asset i , using daily price data, the measure of volatility Vol_{it} is given by:

$$Vol_{it} = \frac{\max(Y_{it}) - \min(Y_{it})}{Y_{it}^C} \quad (1)$$

Where $\max(Y_{it})$, $\min(Y_{it})$ and Y_{it}^C are for time t , the highest, lowest, and closing price. The time series of HLC volatilities are shown in Figure 1² Over time, with the exception of a few spikes, volatility is mostly stable. Outside of these crisis episodes suggesting the existence of intertemporal volatility clusters (see, in particular, Cont, 2007; Mandelbrot, 2013), atypical values are associated with a small number of companies which are always the same over periods of several years. All the volatility series thus obtained show positive skewness. The kurtosis is in all cases higher than 3 (for some series, very high, with a maximum of 276.3). As in the case of fragmentation data, these characteristics are indications of non-linearity, which are in line with the search for a non-linear specification of the effects of fragmentation on the structure of volatility networks.

Starting from the time series of volatilities, we compute the correlation coefficient between assets i and j as:

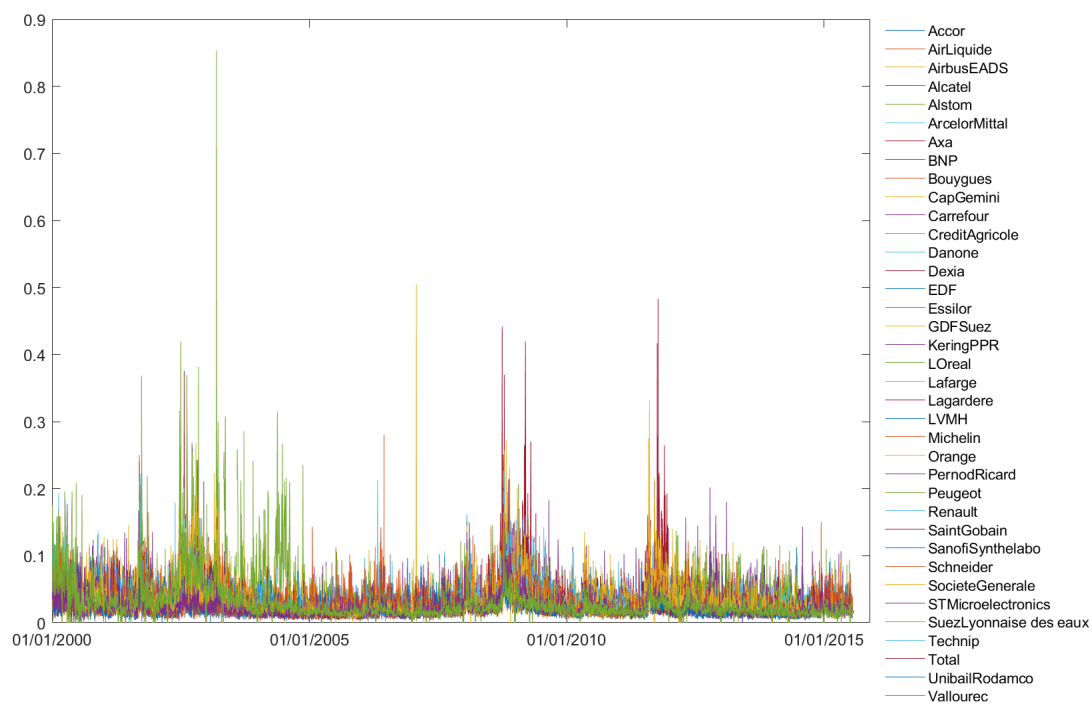
$$\rho_{ij} = \frac{\text{Cov}(Vol_i, Vol_j)}{\sigma_{Vol_i} \cdot \sigma_{Vol_j}} \quad (2)$$

Where: $\text{Cov}(Vol_i, Vol_j)$ is the covariance between volatilities of assets i and j , and σ_{Vol_i} , σ_{Vol_j} their standard deviations. The next step in the development of the minimal spanning tree and hierarchical tree is to transform the correlation matrix into a distance matrix validating the conditions of an Euclidean metric as:

1. $d(i, j) = 0$ if and only if $i = j$

²The full descriptive statistics are provided in appendix in Table III).

Figure 1: **Individual volatilities of the stocks of the sample**
Source: Euronext, authors' calculations



2. $d(i, j) = d(j, i)$
3. $d(i, j) \leq d(i, k) + d(k, j)$

The transformation of the correlation matrix into the unique corresponding suitable distance matrix is achieved using the following distance function (Mantegna, 1999):

$$d(i, j) = \sqrt{2(1 - \rho_{ij})} \quad (3)$$

The set of values of $d(i, j)$ forms the distance matrix D . The unique minimal spanning tree associated to the full distance matrix D and the corresponding hierarchical tree are representations of the subdominant ultrametric associated to this metric. We compute the minimal spanning trees and hierarchical trees using the algorithms of Kruskal (1956) and Prim (1957). The minimal spanning trees and hierarchical trees obtained by this method from correlation matrices of volatilities and providing a network representation of VoV are discussed in section 3.1.

2.1.3 Network indicators

In order to test the empirical relationship between fragmentation and network proxies of VoV, we apply two types of network indicators describing the structure of the minimal spanning trees: distance indicators, and connectivity indicators.³ As regards distances, the first indicator we apply is the average distance to the nearest neighbors, which measures distances within the direct neighborhood of a node. The second distance indicator is the average path length, which measures distances between a node and all the remainder of the network. It is usually considered as one of the most robust distance measures (Newman, 2003). Finally, the heterogeneity of the dynamics of volatilities is assessed using the eccentricity. The eccentricity of a node is the total distance over the longest path from this node to any other node of the network. These three indicators, which characterize the local, average, and maximum distances of the volatility network, are directly related to the VoV: as they decrease, the network becomes denser, i.e. an increase in the common component. At the individual asset level, a reduction in distance is associated with a increase in the common component.

In addition to these three distance indicators, we apply two connectivity indicators: the degree, and the nearest neighbors degree. The degree of a node is the number of edges with which it is directly connected. The average nearest neighbours degree is the average number of neighbours of the nearest neighbours of a node. Both are usual indicators of the position of a node within the global network structure. For example, a hub will generally be characterized by a high degree (number of nodes with which it is directly connected), and a low nearest neighbors degree (number of nodes with which its neighbors are directly connected). A node in the direct neighborhood of a hub will be characterized by a low degree and a high degree of the nearest neighbors

³To save space, we do not detail the calculation of the network indicators. These methods are detailed, for example, in Soramäki et al. (2007).

(since one of them is the hub). Finally a peripheral node will have both a low degree and a low degree of the nearest neighbors. In terms of VoV, the stronger the first- and second-order connectivities of an asset, the stronger the common component of its volatility with a high number of neighbors within the network; and, thus, the less it contributes to the VoV.

In practice, starting from the time series of intraday volatilities, we compute time series of the five network indicators, following Bastidon et al. (2020). The method consists in three steps: first, we compute minimal spanning trees with sliding windows; second, we compute the set of network indicators for each minimal spanning tree; third, we collect the successive values of the set of network indicators in order to get one time series for each network indicator, with the same frequency than the initial database. The time series of network indicators, which are used as dependent variables in the econometric analysis, are presented in Figure 6 at the network level, and in Figure 7 at the asset level, in section 3.

2.2 Modeling the Fragmentation - VoV Relationship

2.2.1 Linear Specification at the Portfolio Level

There exists an emerging literature in which network indicators are used to perform regressions, most of time relying on networks of financial institutions (see for example Chinazzi et al., 2013 for the relationship between the structure of networks of financial institutions and different measures of the severity of the global financial crisis). To the best of our knowledge, this approach is original in the case of networks of assets derived from time series of prices. Using different measures for the VoV that we derive from the network indicators, in this section we model the impact of fragmentation on the VoV at the portfolio level. To this end, we suppose first that the relationship between the VoV and fragmentation is linear and we specify it as:

$$y_t = \alpha_0 + \alpha_1 y_{t-1} + \beta frag_t + \varepsilon_t \quad (4)$$

Where y_t denotes the VoV proxy, $frag_t$ is the fragmentation indicator, α_0 is a constant, α_1 captures further persistence in the VoV dynamics, β measures the fragmentation effect, $\varepsilon_t \rightarrow N(0, \sigma)$ is an error-term.

Model (4) is a transposition at the portfolio level of Hamilton (1979) who assesses the relationship between price efficiency and microstructure characteristics, in particular the number of venues listing each asset, the number of OTC dealers trading each asset, and fragmentation between market venues. This specification is also commonly used in the recent literature, for exemple in O'Hara and Ye (2011) or Gresse (2017) which measure fragmentation with the same type of indicator as the FIDESSA indicator used in the regressions of section 3.

The distance measures at the portfolio level, that is, the average distance to the nearest neighbours (AvDistNN), average path length (AvPathLength) and maximal eccentricity, or diameter, are the most direct proxies of VoV: an increase (respectively,

decrease) in distances at the graph level corresponds to an increase in VoV. The connectivity measures, that is, the standard deviation of degrees (Deg) and average nearest neighbours degree (NNDeg) are also proxies of the VoV in the sense that more (respectively, less) densely connected networks correspond to a decrease (respectively, increase) in the VoV. The choice of these alternative proxies is particularly relevant in order to capture different dimensions of the VoV.

In Model (4), the coefficient β estimates the effect of fragmentation on the VoV in a linear context, under the assumptions of symmetry and linearity. β is a key parameter that estimates the effect of fragmentation on network indicators in a linear context. However, this modeling restricts the relationship between network indicators and fragmentation to be symmetrical and linear. This restriction may be too strong for different reasons. First, just as price dynamics in equity markets may involve multiple regimes, the dynamics of network indicators derived from the same time series of prices could be characterized by non-linearities. In the recent literature, for example, Chan and Santi (2021) characterize speculative bubble dynamics with two regimes; and Jawadi et al. (2018) propose an empirical specification of equity market dynamics where prices are alternatively governed by fundamentals and market sentiment. In the same sense, Zhang (2021) shows that market sentiment, or subjective beliefs, may be essential in generating price and volatility dynamics in equity markets, compared to other market segments where they are not, thus reinforcing the presumption of non-linearity; and Bourghelle et al. (2022) specify a three regime Vector Autoregressive model to describe the bitcoin volatility and show that collective emotions drive well bitcoin volatility. In addition, it is worth to remind that the implementation of the MiFID directive in November 2007 results in the end of monopolies of European stock exchanges and thus market fragmentation, which might imply a time-varying relationship. To better assess this time-variation, we enable hereafter our modeling to include structural breaks and threshold effects, introducing therefore a nonlinear specification.

2.2.2 Nonlinear Specification at the Portfolio Level

In order to take into account this time-variation, we propose to extend Model (4) while including further structural breaks and threshold effects. In practice, this extension enables all coefficients of the above model (α_0 , α_1 and β) to be time-varying. Interestingly, these parameters can take different values according to the level of fragmentation: below the threshold vs. above the threshold. Formally, a two-regime threshold model can be written as:

$$y_t = \left\{ \begin{array}{ll} \alpha_{0,1} + \alpha_{1,1}y_{t-1} + \beta_1 frag_t + \varepsilon_{t,1} & \text{if } S_t < c \\ \alpha_{0,2} + \alpha_{1,2}y_{t-1} + \beta_2 frag_t + \varepsilon_{t,2} & \text{if } S_t > c \end{array} \right\} \quad (5)$$

where: S_t denotes a threshold variable, c refers to the threshold parameter, $\alpha_{0,1}$, $\alpha_{1,1}$ and β_1 are coefficients in the first regime, $\alpha_{0,2}$, $\alpha_{1,2}$ and β_2 are coefficients in the second regime, $\varepsilon_{1,t}$ and $\varepsilon_{2,t}$ are error-terms.

In Model (5), while the parameter β_1 measures the fragmentation effect on the VoV in the first regime, the parameter β_2 captures the time-varying nonlinear effect of fragmentation on the VoV in the second regime. Interestingly, $(\beta_1 + \beta_2)$ measures the global effect of fragmentation on the VoV. Accordingly, the above nonlinear specification can be seen as an On/Off model that includes a threshold effect. Indeed, if the effect of fragmentation is rather linear, only one regime is observed. However, if the fragmentation does enter nonlinearly, our model has the advantage to capture both linear and nonlinear fragmentation effects. Interestingly, the threshold parameter as well as the threshold variables are endogenously identified using the linearity and threshold tests (Hansen, 1996; Tsay, 1989, 1998). Indeed, Model (5) introduces a VoV - fragmentation relationship with two different regimes that are activated when the threshold variable (noted S_t) exceeds a certain threshold, implying a nonlinear relationship between the VoV and the fragmentation index over the whole period, but linear per regime. Indeed, when the transition variable is below the threshold, the market is in a state with low fragmentation, and switches to another state above the threshold.⁴

2.2.3 Linear Specification at the Asset Level

We also perform the specification of the relationship between fragmentation and the VoV at the individual asset level. This approach allows an understanding of the effects of fragmentation on the VoV at the most granular level, that is, at the level of the effects on the contributions of the assets in the portfolio. At the asset level, the standard model that hypothesizes linearity and relates fragmentation and network indicators can be written as:

$$y_{i,t} = \alpha_i + \beta \text{frag}_{i,t} + \gamma \ln(\text{Volume}_{i,t}) + \delta \frac{1}{\text{price}_{i,t}} + \varepsilon_{i,t} \quad (6)$$

Where: $y_{i,t}$ denotes the network indicator for asset i at time t , $\text{frag}_{i,t}$ is the fragmentation indicator, α_i measures individual or fixed effects, β denotes the fragmentation effect, $\text{Volume}_{i,t}$ and $\frac{1}{\text{price}_{i,t}}$ are control variables, γ and δ are coefficients, $\varepsilon_{i,t} \rightarrow N(0, \sigma)$, $i \in [1, N]$, $t \in [1, T]$.

As Models (4) and (5), Model (6) is based on Hamilton (1979) who assesses the relationship between price efficiency and microstructure characteristics. Being specified, like the models typically used in the microstructure literature, at the level of individual assets and not the level of the portfolio, it includes the most usual control variables of these models, that is trading volumes, market capitalizations, and prices in square rate of levels, first differences and/or inverse.

⁴For more details on the properties of this threshold regressions and its modeling steps, the reader can refer to Hansen (1999).

2.2.4 Nonlinear Specification at the Asset level

As in the case of portfolio-level regressions, at the individual asset level, while the linear specification of Model (6) estimates an unconditional β and stipulates that the effect of fragmentation might be time-invariant, this hypothesis is inappropriate given the fact that investors might need time to be familiar with this new mode of organization and trading. Further, the effects of MiFID and of the fragmentation process can be time-varying. Accordingly, an alternative framework to model this time-varying relationship between network indicators and fragmentation can be written as:

$$y_{i,t} = \left\{ \begin{array}{l} \alpha_{1i} + \beta_1 \text{frag}_{i,t} + \gamma_1 \ln(\text{Volume}_{i,t}) + \delta_1 \frac{1}{\text{price}_{i,t}} + \varepsilon_{1i,t} \text{ if } S_t \leq c \\ \alpha_{2i} + \beta_2 \text{frag}_{i,t} + \gamma_2 \ln(\text{Volume}_{i,t}) + \delta_2 \frac{1}{\text{price}_{i,t}} + \varepsilon_{2i,t} \text{ if } S_t > c \end{array} \right\} \quad (7)$$

where S_t denotes a threshold variable; c refers to the threshold parameter; α_{1i} , β_1 , γ_1 , and δ_1 are coefficients in the first regime; α_{2i} , β_2 , γ_2 , and δ_2 are coefficients in the second regime; $\varepsilon_{1i,t}$ and $\varepsilon_{2i,t}$ are error-terms. In the above model, β_1 measures the fragmentation effect in the first regime, while β_2 captures the time-varying nonlinear effect of fragmentation in the second regime. Further, $(\beta_1 + \beta_2)$ measures the global effect of fragmentation.

Model (7) can be seen as an On/Off model that includes a threshold effect in line of Granger et al. (1993). Indeed, if the effect of fragmentation is rather linear, only one regime is observed. However, if fragmentation does enter nonlinearly, our model has the advantage to capture both linear and nonlinear fragmentation effects. Indeed, Model (7) is a nonlinear model that captures the linear effect of fragmentation (β_1) and the nonlinear effect of fragmentation (β_2). This modeling has the advantage to enable us to assess for time-variation of the fragmentation effects that vary by regime. In particular, while beta (β_1) captures the fragmentation effect in the regime 1 when the threshold variable is under the estimated threshold and beta (β_2) captures the fragmentation effect in the upper regime, the overall effect of fragmentation is provided by the sum of (β_1) and (β_2). This is also an intrinsic property of this class of threshold model (Granger et al., 1993; Terasvirta et al., 2010).

From an econometric point of view, this model does belong to the class of threshold models introduced by Lim and Tong (1980) and extensively discussed in Tong (1990). It proposes a specification with two different regimes activated when the transition variable⁵ exceeds a certain threshold, implying a nonlinear relationship between network indicators and the fragmentation index over the whole period, but linear per regime. Indeed, when the transition variable is below the threshold, the market is in a state with low fragmentation, and switches to a state with high fragmentation above the threshold. Obviously, the above specification might be extended when considering more than two regimes.

⁵According to Tsay (1986, 1989) and Hansen (1996), the optimal transition variable is that for which linearity is the most strongly rejected.

This model has different advantages. First, it offers flexibility to model time-varying fragmentation effects. Second, it enables fragmentation elasticity to vary over time with the change in market adjustments while allowing for nonlinear and asymmetric adjustments. Third, compared to other switching models, our model has the advantage of endogenously estimating the thresholds and identifying the regimes.

3 Results and discussion

In this section, we first present and discuss the structure of the volatility networks (section 3.1). Then we present and discuss the econometric results using the VoV proxies at the portfolio level (section 3.2), and the econometric results using the VoV proxies at the individual asset level (section 3.3).

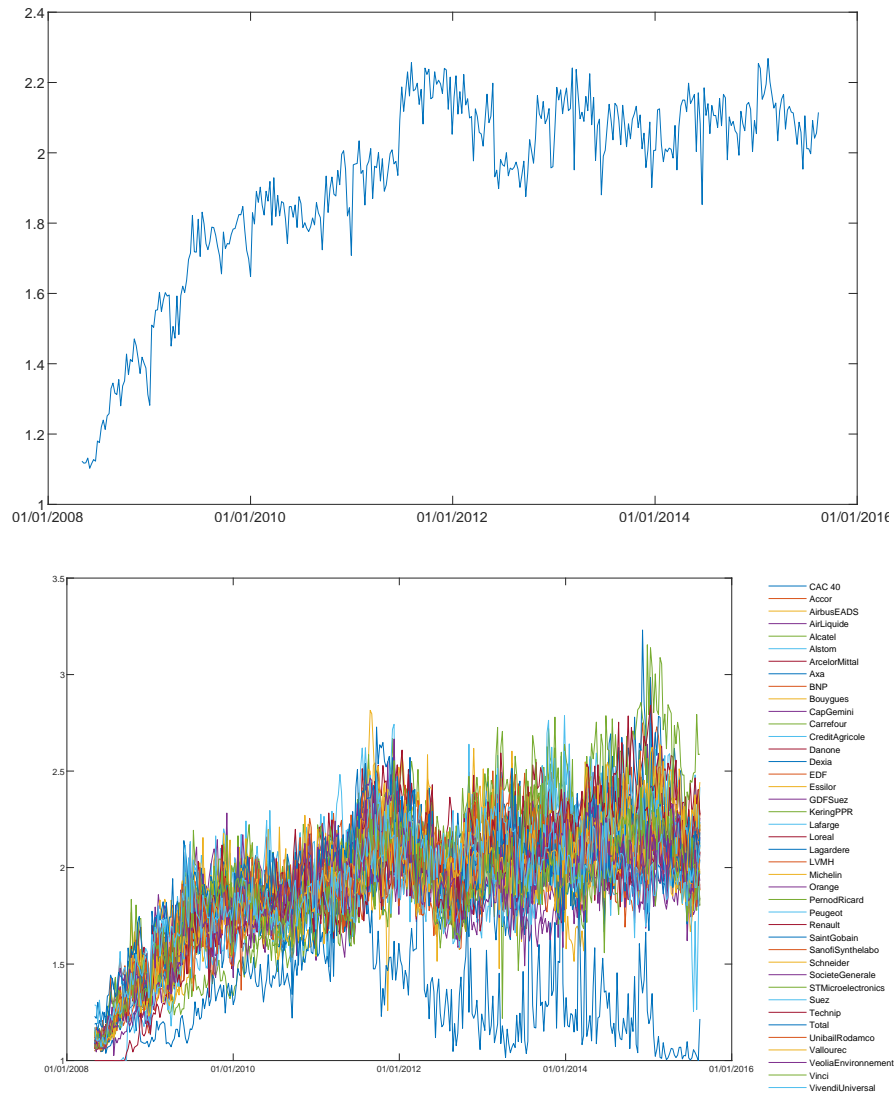
3.1 Structure of volatility network representations

3.1.1 Trades fragmentation data

The study assesses the relationship between fragmentation and the structure of French equity market volatility networks. Fragmentation between the different market venues exhibits partly specific dynamics from one country to another (He et al., 2015). The French market is representative of the fragmentation of European markets, roughly at the same level as Germany or the United Kingdom (CBOE, 2022a). The database starts in 2000 and ends in 2016. Since MIFID is implemented at the end of 2007, it is chosen to span an equivalent duration before and after the regulatory shock. The network representations presented in Section 3.1 cover the pre-MIFID period, as a benchmark, and the post-MIFID period. The econometric study of the relationship between fragmentation and the VoV presented in Section 3.2, at the portfolio level; and in Section 3.3, at the individual asset level, covers the post-MIFID period. This period corresponds to a period of rapid progression of fragmentation, followed by a period of stabilization. The level of fragmentation has remained stable since then.

In order to assess the relationship between market fragmentation and volatility in a network perspective, it is necessary to select, at the asset level, measures of market fragmentation, besides measures of the position of assets within the network. Two types of fragmentation data are available. The first type of data, provided by CBOE, which is itself one of the venues in the European Union’s equity markets, is in the form of market shares per venue. However, these data are available only at the aggregated level for marketplaces, and not for individual assets. The second type of fragmentation data is provided by FIDESEA, a software and trading information systems provider, from May 2008 onwards. These data are available for national benchmark indices, but also at the asset level. In all cases, the FIDESEA index associated with a given asset corresponds to the inverse of the Herfindhal index of the market shares of the different venues trading this asset. In other terms, a FIDESEA index of 1 indicates no fragmentation. The higher the index, the higher the fragmentation of trades between market venues.

Figure 2: **FIDESSA fragmentation index**



(a) Fragmentation index, CAC40 index; (b) Fragmentation index, individual asset level. Source: weekly fragmentation data provided by FIDESSA

The CAC40 fragmentation data are represented in Figure 2(a), and the individual fragmentation data of the portfolio in Figure 2(b).⁶ The composition of the index varying over time during the study period, we take into account the assets that are part of it for at least a quarter of the period, and for which there are available fragmentation data, that is a total of 39 assets. A visual inspection of the fragmentation of trades on the CAC40 index (Figure 2(a)) shows two sub-periods: a first sub-period corresponding to the rise in the fragmentation of trading till July 2011, and a second sub-period of stabilization after this rise. Interestingly, this corresponds to the dates of the structural breaks in the individual topological distance indicators presented in Table 4.

Individual fragmentation data (Figure 2(b)) show that fragmentation levels within the portfolio tend to diverge. However, regardless of the date considered, only a small number of assets show truly atypical values, and these assets are always the same. Dexia (banks)⁷, in great difficulty during the 2008 and 2011 crises, diverges with an atypically low fragmentation over almost the whole period when fragmentation data are available, with a fragmentation of trades being often close to the lower bound. Lafarge (construction & materials) also diverges in the context of a controversial merger at the very end of the study period.

Even not taking these atypical assets into account, fragmentation levels within the portfolio tend to individualize over time. Initially between about 1 and 1.3, the index shows a maximum dispersion (between about 1.7 and 3.2) at the end of 2014 and the beginning of 2015. Otherwise, during the period of stabilization of fragmentation, the minimum values are generally of about 1.6 and the maximum values of about 2.5 to 2.7. We note that, with the exception of three assets, all series show negative skewness. The kurtosis is between 1.8 and 5.2 (greater than 3 for 29 out of 39 series). These characteristics are indications of non-linearity, which justify the search for a non-linear specification of the effects of fragmentation.

Given the absence of market fragmentation before MiFID, in the following we discuss the structure of volatility networks, in relation with the measurement and visualization of the VOV, using three subperiods: a first sub-period without fragmentation, prior to the adoption of MiFID (2000/01-2007/11); a second sub-period corresponding to the rise in fragmentation (2007/12-2011/07); and a third sub-period corresponding to the stabilization and divergence of fragmentation (2011-07/2015). It has to be noticed that there are no data on the market shares of the different venues before 2008/05, which is the first datapoint in the FIDESSA dataset. Thus the split between the first and second subperiod is fixed at the date of the regulatory shock introducing competition.

⁶The full descriptive statistics are in appendix in Table I)

⁷All sectors in the paper refer to the Industry Classification Benchmarks (ICB), which is the most commonly used standard for the categorization of companies by industry within equity markets indices. For details, see Table II in appendix.

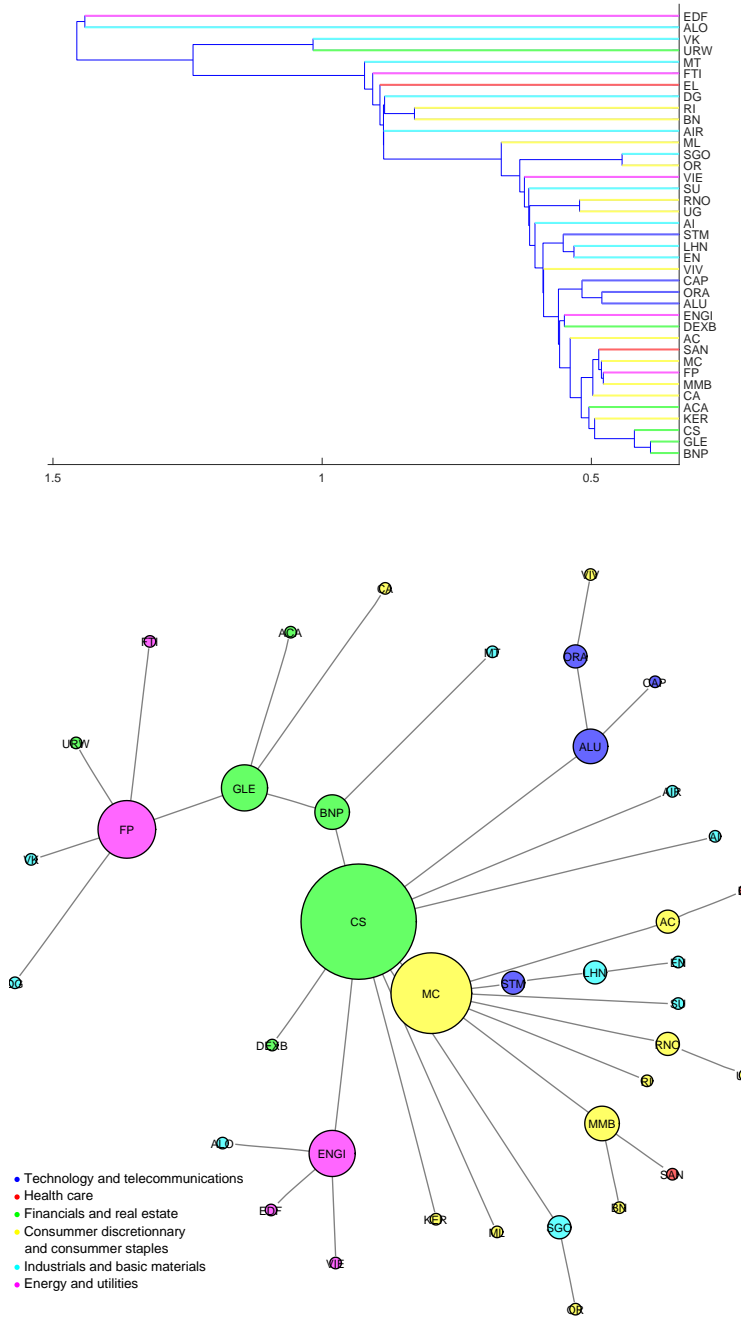
3.1.2 Volatility network representations, before market fragmentation

As stated previously both minimal spanning trees and hierarchical trees display specific informations: the hierarchy of distances in *hierarchical trees* allows to compare to the degree of similarity of time series of volatility of each stock relative to the rest of the sample. The shortest the distance, the highest the similarity; and to the contrary, the longest the distance, the more the time series of volatility is diverging in comparison with the remainder of the sample and contributing to the VOV. *Minimal spanning trees* especially provide information on the structure of the network, the hubs, and the composition of sub-groups. They thus reveal the structure of the VoV: the branches of the tree are a visual representation of the divergence of volatilities.

The hierarchical tree of the first sub-period shows four groups of stocks (Figure 3a). The first cluster, from BNP to SAN (Sanofi), with the shortest distances, includes all the hubs of the backbone of the minimal spanning tree, from FP (Total, Energy and utilities) to MC (LVMH, Consumer discretionary and staples). Three financial stocks are at the center of the chain (BNP; GLE, Société Générale; CS, Axa). In addition this first cluster includes an handful of assets in direct connexion with the hubs, mainly from the sector of Consumer discretionary and consumer staples (KER, KeringPPR; CA, Carrefour; MMB, Lagardere). A second group of stocks is connected with slightly higher distances. From AC (Accor) to ML (Michelin), it is mainly composed of stocks from the sectors of Technology and telecommunications, Consumer discretionary and staples and Industrial and basic materials. To the contrary, the third group of stocks (from AIR, Air Liquide; to VK, Vallourec) and to a greater extent the fourth group (ALO, Astom and EDF) are connected with highly superior distances. Those two groups are characterized by a higher proportion of stocks from the sector of Industrials and basic materials than the second group (the first cluster including none). The last group has the peculiarity of being solely composed of two main electricity providers which were partly held by the French government at this date.

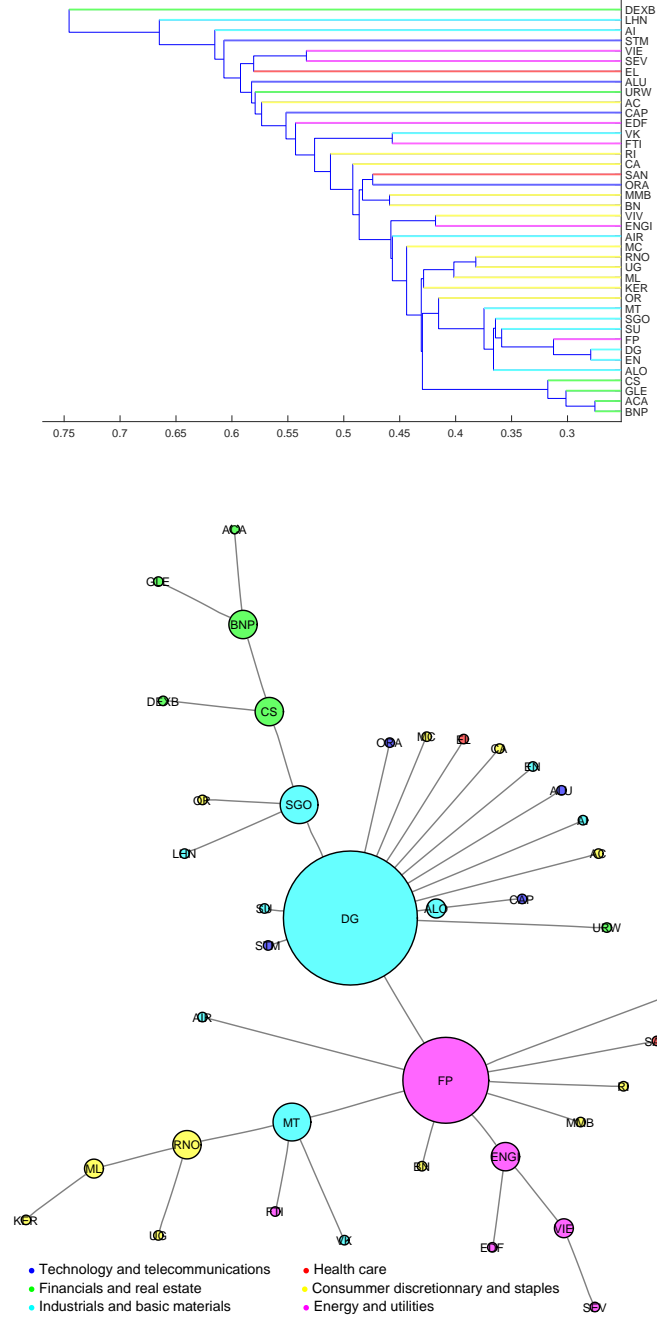
As stated previously, this hierarchical tree is associated with a minimal spanning tree (Figure 3(b)) which backbone is composed of a chain of hubs. The most central is CS (Axa, Financials and real estate: insurance), BNP (Financials and real estate: banks) and GLE (Société Générale, Financials and real estate: banks) being less connected but also belonging to the chain. This first minimal spanning tree emphasizes the central position of financial stocks within the volatility network. The sectors related to household consumption are located in intermediate zones of the network, while those related to industrial activities remain peripheral. The sector of Energy, which activity is partly of industrial nature, has the peculiarity of being both characterized by a relatively high connectivity and a relatively peripheral position.

Figure 3: **Topology of the sample, sub period 1**



(a) Hierarchical tree, (b) Minimal spanning tree, distance measures à la Mantegna (1999). For the minimal spanning tree, the diameter of the nodes is proportional to their degree. For both representations, the colors corresponds to the ICB sectors (1 digit) and the companies are named by their tickers. The detail of the sectors and tickers is shown in Table II.

Figure 4: **Topology of the sample, sub period 2**



(a) Hierarchical tree, (b) Minimal spanning tree, distance measures à la Mantegna (1999). For the minimal spanning tree, the diameter of the nodes is proportional to their degree. For both representations, the colors corresponds to the ICB sectors (1 digit) and the companies are named by their tickers. The detail of the sectors and tickers is shown in Table II.

3.1.3 Volatility network representations during the first phase of rise in market fragmentation

During the second sub-period, which follows the implementation of MiFID, the hierarchy disclosed by the hierarchical tree (Figure 4(a)) of distances associated with the Industrials and basic materials and the Consumer discretionary and staples sectors reverses. While there were previously stocks of the later connected with distances ranking just after financial stocks in the first cluster, there is now a notable difference in distances between OR (L'Oréal), the shortest distance of the sector of Consumer discretionary and staples, and the pair DG - EN (Vinci - Bouygues, Industrials and basic materials), which is connected by one of the lowest distances within the sample. In general, the stocks from the Industrials and basic materials sector are characterized by a wide range of distances, while the sector of Consumer discretionary and staples is connected with medium distances. The financial sector remains characterized by the shortest distances.

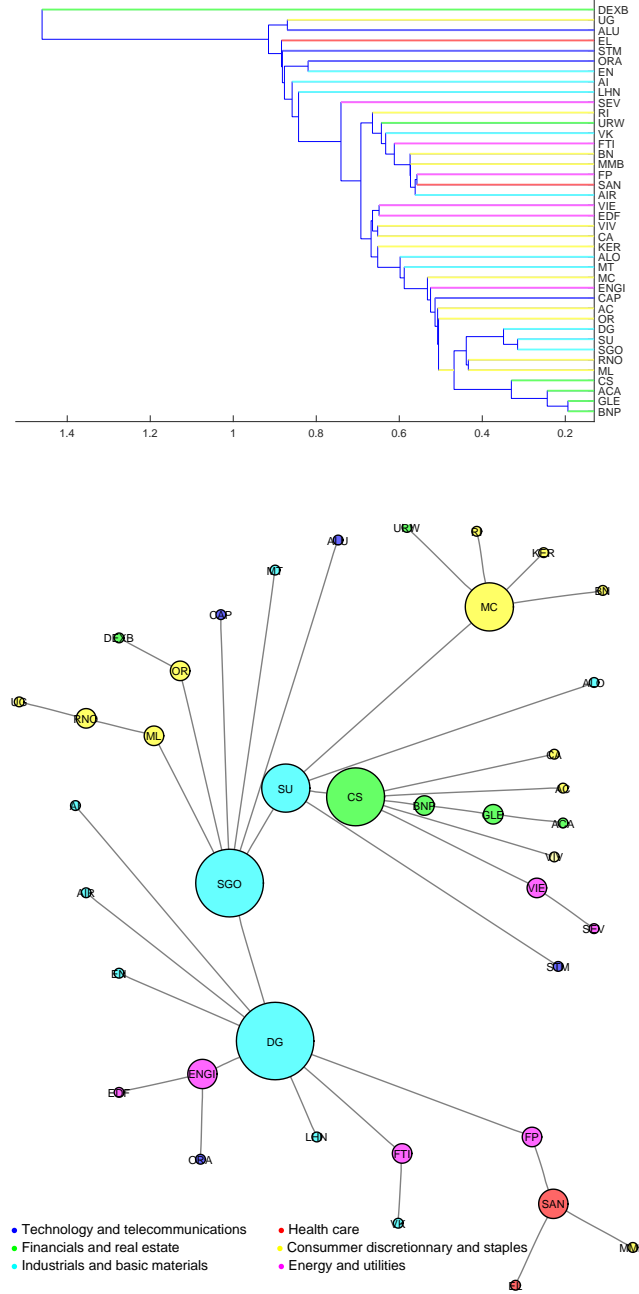
The reversal of the hierarchy of distances is also found in connectivities within the minimal spanning tree (Figure 4(b)), now structured around a main hub (DG: Vinci, Industrials and basic materials) and a secondary hub (FP: Total, Energy and utilities). Financial and real estate, on the one hand; and Consumer discretionary and staples, on the other hand, are located in peripheral branchings. In general, the network of volatilities in this second sub-period differs from the first in that the financial sector is much less central (even though the assets in this sector remain connected to each other by very small distances), the industrial sector is much more central, and the sectoral grouping of assets in the different branchings is even more evident. The hierarchy of sectoral contributions to the VOV is then presumably not drastically different from the pre-fragmentation period, but it is notably affected.

3.1.4 Volatility network representations during the stabilization of market fragmentation

The hierarchical tree of the third sub-period (Figure 5(a)), which corresponds to the stabilization of trades fragmentation, is relatively similar to that of the second. Financial stocks remain connected by the shortest distances. The distances by which the stocks from the sector of Industrials and basic materials are connected to the network are superior to the average; while the distances by which the stocks from the Consumer discretionary and staples are connected are inferior to the average. Both sectors are characterized by a large heterogeneity. The sector of Energy and utilities is connected with medium distances, and the sectors of Technology and telecommunications and Health care are connected with high distances.

As regards the minimal spanning tree (Figure 5b), the backbone is composed of a chain of hubs, as in the first sub-period. Three of these hubs, of which the two main ones (DG, Vinci; and SGO, Saint-Gobain), are from the Industrials and basic materials domain. The two last hubs, located at the end of the chain, are MC (LVMH, Consumer discretionary and staples) and CS (AXA, Financials and real estate).

Figure 5: **Topology of the sample, sub period 3**



(a) Hierarchical tree, (b) Minimal spanning tree, distance measures à la Mantegna (1999). For the minimal spanning tree, the diameter of the nodes is proportional to their degree. For both representations, the colors corresponds to the ICB sectors (1 digit) and the companies are named by their tickers. The detail of the sectors and tickers is shown in Table II.

In general, the volatility network remains primarily structured around Industrials and basic materials stocks, with stocks from other sectors connected in part (Consumer discretionary and staples) or in full (Financials and real estate) by short distances being grouped together in branchings outside the backbone. Overall, the structure of volatility networks and the hierarchy of the VOV contributions continue to show a highly visible sectoral grouping. At the margin, the position of sectoral asset groups and their place in the hierarchy vary.

Ultimately, two methodological remarks can be made. First, the topological representations presented above are validated by economic interpretation. Both hierarchical trees and minimal spanning trees of volatilities are organized based on economic sectors, which is not self-evident given the diversity of investment strategies of market participants in fragmented equity markets, particularly the rise in high frequency trading. In particular, the gap between the common component of the volatility of financials stocks and the rest of the sample remains large over sub-periods. Yet, their topological importance tends to be reduced. Financial stocks provide one hub and two secondary hubs in sub-period 1, but they are reduced to peripheral branchings or sub-trees in sub-periods 2 and 3. This likely reflects a decreasing VoV of these stocks together but not necessarily with the rest of the sample. This is valuable information both for investors holding portfolios of financial sector securities, and for public authorities, particularly in a context where credit risk spillovers between the financial sector and sovereigns are disrupted by major episodes of financial strains and subsequent bailouts (Greenwood-Nimmo et al., 2019). Our findings suggest that a strong support to a distressed bank is both legitimized by the decreasing intra-sectoral VoV, and less necessary because of a reduced inter-sectoral VoV.

The second remark is that the network position (low distances, high connectivity) of the stocks of the sample appears not to be always related to their market capitalization, which is usually a highly significant control variable of the effect of fragmentation on the liquidity and volatility of individual stocks. Among the two main capitalizations, Sanofi (SAN, Health care) is never a hub, and Total (FP, Energy and utilities) only in sub-period 2. To the contrary, AXA (CS, Financials and real estate), LVMH (MC, Consumer discretionary and staples) and Vinci (DG, Industrials and basic materials) in particular, which market capitalizations are much less important, are much more central in volatility networks. This suggests that the relevant control variables in the assessment of the individual effects and network effects of fragmentation may differ. For this reason we enter the price and volume variables separately in the tests of section 3.3.

The purpose of the next sections is an attempt to identify empirical relationships between indicators of the structure of these network representations, used as alternative VoV proxies, and fragmentation, and to provide a discussion in light of the VOV literature. In Section 3.2, the relationship is tested at the aggregated portfolio level. In Section 3.3, it is tested at the individual asset level with panel data.

Table 1: **Results of structural Break Test**

Test	AvdistNN	Avpath	Deg	ECC	NNdeg
n	2	0	2	3	2
Date of Break	14/07/2010	—	19/10/2010	05/01/2011	25/7/2011
—	12/08/2011	—	28/09/2012	28/09/2012	28/09/2012
—	—	—	—	31/06/2014	—

Note: n indicates the number of breaks

3.2 Modeling the Fragmentation - VoV Relationship at the portfolio level

3.2.1 Structural breaks tests

For the analysis at the portfolio level, we use the fragmentation data for the CAC40 portfolio and the VoV network proxies at the graph level. The analysis of Figures 2(a) presenting fragmentation data and 6(a) to 6(e) presenting the network proxies of VoV shows that all series appear to be stationary. This result is confirmed by the Unit Root tests (ADF, 1979, 1981) tests and Phillips and Perron (1988) tests⁸. Second, Figures 6(f) and 6(g) show further evidence of time-variation in the dynamics of VoV and fragmentation indices. Indeed, from Figure 6, it seems that the the reaction of VoV to fragmentation varies with the progress of the fragmentation process, which might suggest further time-variation in the fragmentation - VoV relationship. This time-variation might be indication of structural breaks and non-linearity, which escape the linear model and can justify the weak level of linear unconditional correlations.

In order to check this time-variation property, we applied a structural break test of Bai and Perron (2003) that allows for maximum of five breaks. Interestingly, these breaks are determinated endogenously. We present the main results of this test in Table 1. Accordingly, we find that except for the proxy Avpath, the results point to the presence of multiple breaks in the VoV dynamics. This result is inline with the time-variation mentionned in our preliminary analysis.

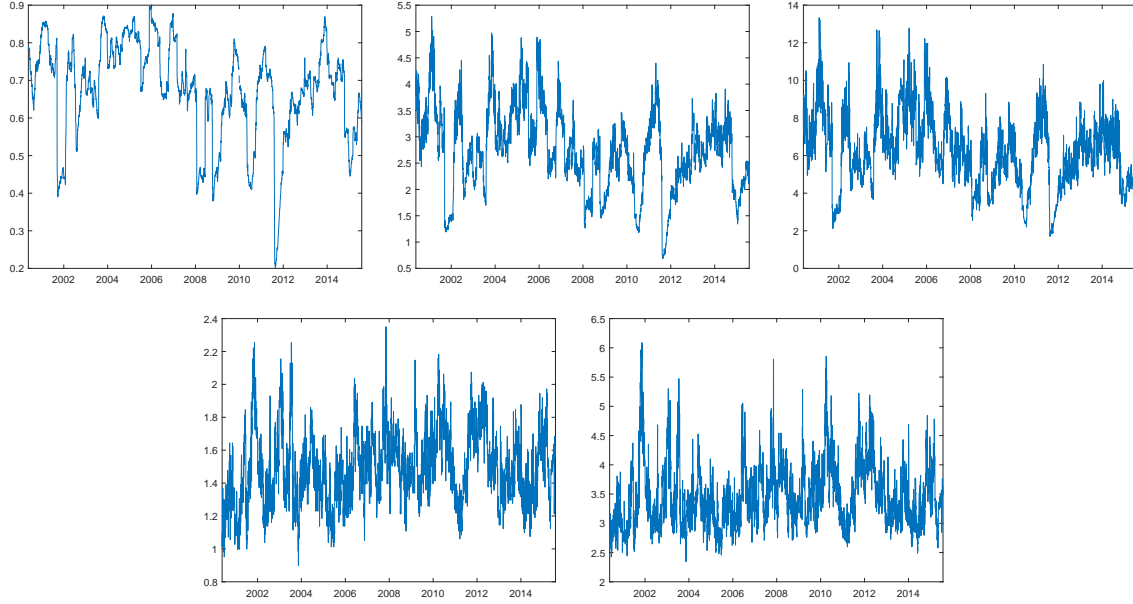
3.2.2 Results of VoV regressions

Netx, we consider Model 5 for which all coefficients are being time-varying across regimes and which extends Model 4 to a nonlinear framework. We report the main results in Table 2.

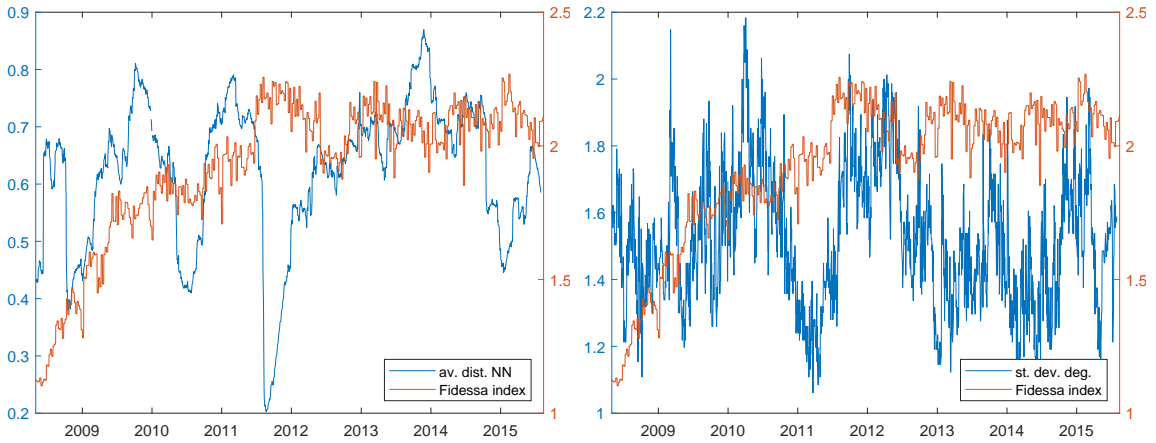
From Table 2, we note different interesting results. First, at the most general level, whatever the proxy for the VoV, we show further evidence of significant persistence

⁸We do not report the results of unit root tests to save space, but these results are available upon request.

Figure 6: Volatility networks indicators, graph level



(a) Average distance to the nearest neighbours, (b) average path length, (c) diameter (maximal eccentricity), (d) standard deviation of degrees, (e) average nearest neighbors degree.



(f) Average distance to the nearest neighbours vs. Fidessa index CAC40, (g) standard deviation of degrees vs. Fidessa index CAC40.

Table 2: Results of VoV Regressions

$$y_t = \begin{cases} \alpha_{0,1} + \alpha_{1,1}y_{t-1} + \beta_1 \text{ frag}_t + \varepsilon_{t,1} & \text{if } S_t \leq c \\ \alpha_{0,2} + \alpha_{1,2}y_{t-1} + \beta_2 \text{ frag}_t + \varepsilon_{t,2} & \text{if } S_t > c \end{cases}$$

Coefficients	AvdistNN	Avpath	Deg	Ecc	NNdeg
Regime 1					
$\alpha_{0,1}$	0.006*** (0.02)	0.064*** (0.01)	0.155*** (0.00)	0.412*** (0.01)	-0.364*** (0.00)
$\alpha_{1,1}$	0.991*** (0.00)	0.978*** (0.00)	0.846*** (0.00)	0.919*** (0.00)	0.890*** (0.00)
β_1	-0.003*** (0.03)	-0.005*** (0.00)	0.053*** (0.00)	0.004 (0.96)	0.010 (0.73)
n_1	572	1883	641	697	838
$S_{i,t}$	$\text{frag}_{i,t}$	—	$\text{frag}_{i,t}$	$\text{frag}_{i,t}$	$\text{frag}_{i,t}$
Regime 2					
$\alpha_{0,1}$	0.069*** (0.00)		-0.104 (0.13)	2.80*** (0.00)	0.258 (0.31)
$\alpha_{1,1}$	1.01*** (0.00)		0.890*** (0.00)	0.913*** (0.00)	0.791** (0.00)
β_1	-0.041*** (0.00)		0.135*** (0.00)	-1.14*** (0.00)	0.276*** (0.03)
n_2	282		506	450	309
Regime 3					
$\alpha_{0,1}$	-0.012 (0.13)		0.050 (0.59)	2.72*** (0.00)	0.118 (0.63)
$\alpha_{1,1}$	0.959*** (0.00)		0.829*** (0.00)	0.761*** (0.00)	0.826*** (0.00)
β_1	0.007*** (0.03)		0.094*** (0.03)	-0.535 (0.14)	0.221** (0.05)
n_3	1029		736	445	736
Regime 4					
$\alpha_{0,1}$				2.70*** (0.00)	
$\alpha_{1,1}$				0.893** (0.00)	
β_1				-1.016** (0.03)	
n_4				291	
R^2	0.94	0.95	0.79	0.87	0.79
$F - Test$	0.00	0.00	0.00	0.00	0.00

Note: R^2 denotes the R-squared. n_i (for all $i = 1, \dots, 4$) denotes the number of observations per regime.

(***), (**), and (*) denote significance at the 1%, 5%, and 10% levels, respectively. Values in () are the p-values of estimators with White cross-section standard errors & covariance.

in the dynamics of VoV. Second, we find that except for the average path length, the assumption of switching regime is validated as the relationship between fragmentation and VoV exhibits asymmetry and nonlinearity, confirming the time-variation property that we mentioned in the preliminary analysis. Third, we find that when considering the fragmentation effect on the VoV, except for the average path length proxy, fragmentation has not only a significant effect on VOV but also its effect enters nonlinearly and varies with the regime under consideration.

Let us recall that according to the microstructure theoretical literature, effective competition (and thus fragmentation) enhances the efficiency of the price formation process. If this effect is common to all stocks, then we would expect a negative effect of fragmentation on VOV. However, fragmentation measured at the index level may reflect divergent individual fragmentations. In this case, even if the theoretical efficiency-enhancing hypothesis is validated, because the aggregated fragmentation index reflects divergent fragmentations, the effects on individual volatilities are also divergent, and one can imagine a positive aggregated effect of fragmentation on VoV. This effect is only likely to emerge if the relationship between fragmentation and VoV is tested at the portfolio (for fragmentation) and graph (for VoV proxies) levels, and not in panels with individual measures. For the proxies we retain, for the distance measures that are the most direct proxies of VOV (*AvdistNN*, *Avpath*, *Ecc*), the expected effect is therefore generally negative (possibly positive at the end of the period). For the connectivity measures, it is positive (possibly negative at the end of the period).

For the average distance to the nearest neighbours proxy (*AvdistNN*), we identify three different regimes. In the first two regimes, as expected, we find that the fragmentation effect is negative and significant (slightly higher in the second regime), while it is lower in its absolute value and positive in the third regime. These successive negative and positive effects are in line with the microstructure literature. The negative effect of fragmentation is related to the competition across financial markets that yields more efficiency and therefore provides a reduction in individual volatilities. The positive effect in the third regime is explained by further heterogeneity in fragmentation across the financial assets of the CAC40, possibly associated with an attenuation of the fragmentation effect. For the two other proxies of VoV based on distance measures, the effect of fragmentation is always negative. These results are particularly interesting since the average path length (*Avpath*) and eccentricity (*Ecc*) are aggregated distances, and thus specifically characterize the whole graph and non local parts, unlike the distance to nearest neighbors. When considering the average path length, we find only one regime and it appears that fragmentation has a negative and significant effect on VoV, which does suggest that *a priori* competition affects the contribution to the VoV of individual financial assets with the same manner and speed. For the eccentricity proxy, our structural tests point to four regimes, the effect of fragmentation on VoV not being significant in the first regime, and then always negative.

For the connectivity proxies (standard deviation of degrees, *Deg*; and degree of the nearest neighbours, *NNdeg*), we identified three regimes. With the exception of the first regime for the nearest neighbours degree (where it is insignificant), market

fragmentation has a positive and significant effect on the VoV which is in line with the theoretical literature.

Overall, at the portfolio level, our estimates show that fragmentation has a time-varying and nonlinear effect on the VoV that varies per regime. In particular, while a negative impact of market competition on VoV is expected and suggests that fragmentation has improved market efficiency and reduced volatility, a positive effect is also an interesting finding as it results from the heterogeneity associated with the fragmentation that is captured by local distances. This effect appears specifically with the nearest neighbours distances and at the end of the period, which shows the interest of using several VoV proxies and a non-linear specification. In the next section, we explore the relationship between fragmentation and network indicators as proxies of the contributions to the VoV using panel data at the asset level, in order to shed light on the effects of heterogeneity in fragmentation dynamics.

3.3 Modeling the fragmentation - VoV relationship at the asset level

The nonlinear model in equation (7) is a particular case of an abrupt threshold Autoregressive (TAR) model. Accordingly, it can be estimated using a similar econometric strategy based on the sequential conditional least square method of Tong and Lim (1980) discussed by Tsay (1989, 1998) and Hansen (1996). This strategy identifies three main steps: i) specification, ii) estimation and iii) validation. Tsay (1989) and Hansen (1996) developed specific procedures using threshold tests to specify the value of the threshold c while testing the null hypothesis of linearity against its nonlinearity alternative. In particular, Tsay (1989) and Hansen (1996) introduced two linearity test strategies. Tsay (1989) proposed a linearity test related to Petrucci and Davies (1986) Portmanteau test of nonlinearity based on the arranged regression and predictive residuals. Tsay (1989) test is a combination of Keenan (1985), Tsay (1986), and Petrucci and Davies (1986) linearity tests. Hansen (1996) allows for a more global strategy, while suggesting that c can be determined according to Tsay (1989)'s principle.

In practice, we apply hereafter both tests to check the robustness of our results. In particular, we rely on threshold and linearity tests to check for nonlinearity in the data and to test the presence of a threshold effect in the data. When linearity is rejected and our tests conclude in terms of the threshold regression, we identify the different regimes. Finally, for each regime, we estimate parameters, and we apply different misspecification tests to check the robustness of our findings.

Before moving to the application of these tests, we recall briefly the modeling steps of the threshold market model. First, the estimation of the threshold model requires the application of sequential conditional least squares only. As in Tong and Lim (2009), the TAR modeling is carried out in three main steps, which consist of specifying further lags in the model, defining the threshold parameter c and the threshold variable and estimating the two-equation system by the Least Squares (LS) method. However, as the value of threshold is unknown, Tsay (1989) and Hansen (1996) introduced a procedure

based on linearity tests. In particular, one should first apply threshold tests to specify the value of c , while testing the null hypothesis of linearity against its non-linearity alternative. If linearity is rejected, one can specify the different regimes according to the pre-defined threshold parameter. Next, the regressions are estimated for each regime.

3.3.1 Dependence Tests

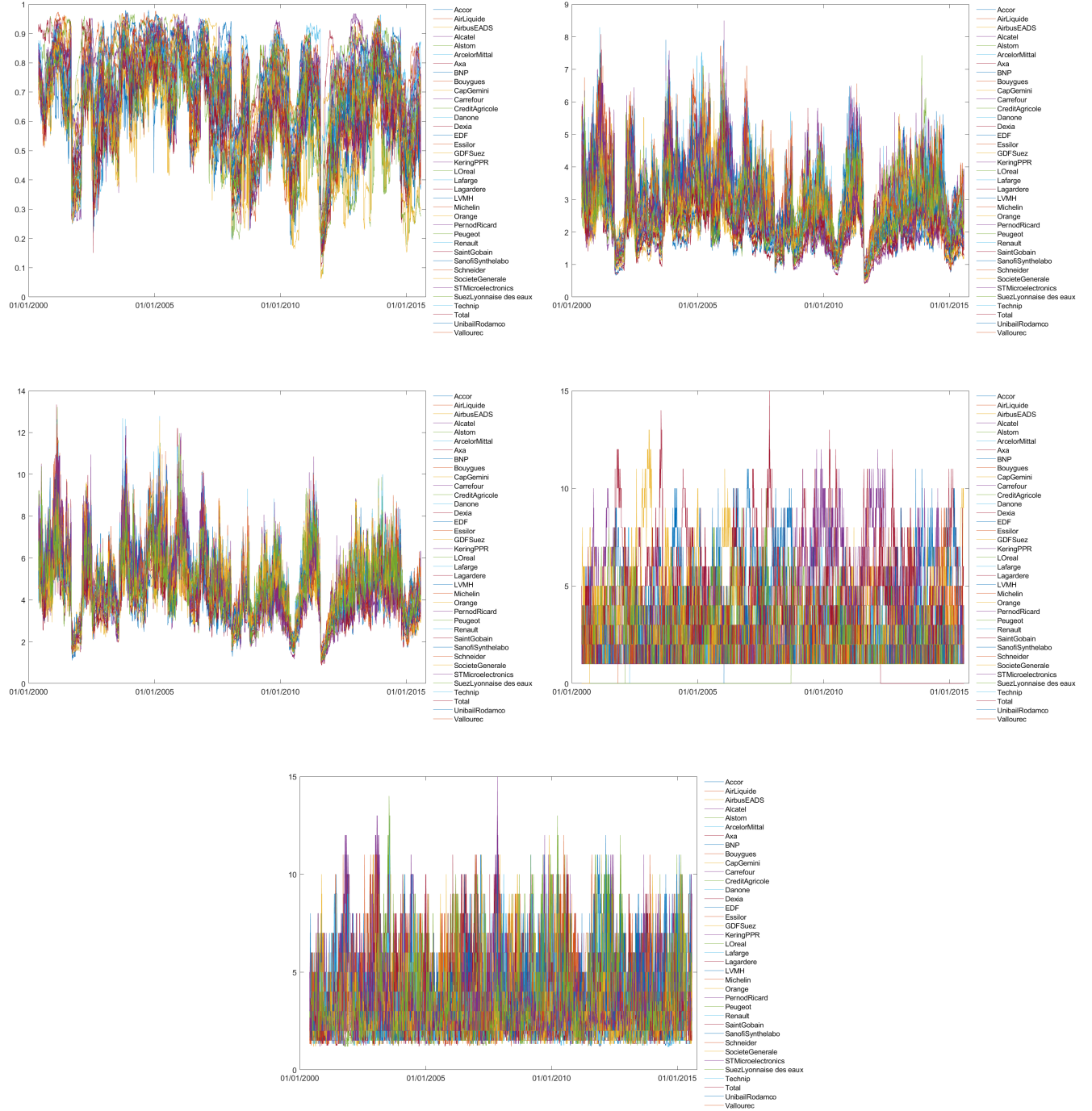
For the analysis at the individual asset level, we use both fragmentation data and the VoV network proxies at the asset level. The time series of fragmentation data are presented in Figure 2b and the VoV network proxies are in Figure 7.⁹ In general, distance measures tend to increase till 2006, then decrease till 2011 and finally increase again with a strong divergence. Within this general trend, 2011 exhibits a peak for all distance measures. Over the whole period considered, the maximum values of the average and maximum distance measurements are decreasing, pointing to a densification of the network. The hierarchies of distances are generally stable over time. The hierarchies of connectivities are less stable, which illustrates the absence of a permanent hub. These preliminary observations are already relevant insofar as they allow the identification of the overall pattern of VoV. Moreover, to the extent that distance hierarchies are rather stable and some assets have persistently high connectivities, the hierarchy of contributions to VOV is also presumably rather stable.

We carry out several dependence tests to check whether these network indicators exhibit further dependence or not. The aim is to test the null hypothesis of independence against a further dependence in the dynamics of volatility. In particular, when the dependence hypothesis is not rejected, these tests enable us to double check whether this dependence is linear or not. These tests are required in order to check whether the dynamics of network indicators present a further dependence structure or not. Also, these tests are always applied before linearity tests. To this end, we apply Breusch and Pagan (1980) LM test, Pesaran (2004) scaled LM test and Baltagi et al. (2012) bias-corrected scaled LM, which test the null hypothesis of No cross-section dependence against a further dependence in the data. The main results of these tests, reported in Table 3, indicate the rejection of the null hypothesis, suggesting further dependence in the data under consideration.

This result is relevant and can be justified by the presence of common shocks across the sectors under consideration. In particular, within the fragmentation of trades and the implementation of MiFID it is possible that these common regulatory shocks have yielded an increasing financial integration across French stocks. This is also in line with the above findings in terms of interactions between stocks and the dynamics of network indicators of distance and connectivity. Next, we check whether the dynamics of these network indicators exhibit further breaks.

⁹For the corresponding descriptive statistics, see Table IV in Appendix.

Figure 7: Volatility networks indicators, individual asset level



(a) Average distance to the nearest neighbours, (b) average path length, (c) eccentricity, (d) degree, (e) nearest neighbors degree.

Table 3: **Results of Dependence Tests**

Test	AvdistNN	Avpath	Deg	ECC	NNdeg
<i>Breusch – Pagan LMtest</i>	0.00***	0.00***	0.00***	0.00***	0.00***
<i>Pesaran scaled LM test</i>	0.00***	0.00***	0.00***	0.00***	0.00***
<i>Bias – corrected scaled LM test</i>	0.00***	0.00***	0.00***	0.00***	0.00***

Note: Values reported indicate the pvalue of the tests. (***) denotes rejection of the null hypothesis at 1% statistical level.

Table 4: **Results of structural Break Tests**

Test	AvdistNN	Avpath	Deg	ECC	NNdeg
n	1	1	1	1	1
<i>Date of Break</i>	t 12/08/2011	17/08/2011	30/07/2014	10/10/2011	05/04/2012

Note: n indicates the number of breaks.

3.3.2 Structural Break Tests

We check for the presence of further structural breaks in the data. To this end, we apply Bai and Perron (2003)’s test for multiple breaks. We conduct this test to determinate sequential breaks to a maximum of five. We present the key results of this test in Table 4.

Overall, our analysis points to the presence of significant structural breaks for all network indicators. The presence of significant breaks shows that the dynamics of these indicators might exhibit threshold effects. Accordingly, the dynamics of network indicators is not correctly reproduced using linear models such as Model (6). Next, we check whether the nonlinearity option can be used to improve the model and estimate the effect of fragmentation using linearity and threshold tests.

3.3.3 Linearity and Threshold Tests

When data exhibit breaks, the relationship could be nonlinear. In particular, this might indicate further instability. This instability can be due to the fact that the dynamics of the data shows different states and regimes. The existence of different regimes does mean that the model that generates the data may show nonlinearity and/or threshold effects such that its coefficients may take different values that vary per regime and according to the activation of a given threshold. To account for this phenomenon, we apply the Hansen and Tsay tests to check linearity against nonlinearity and switching regimes, which assume an abrupt transition between regimes. We report the main results in Table 5.

From Table 5, we note that all linearity tests confirm our previous findings as linear-

Table 5: **Results of Linearity Tests**

	Tests	AvdistNN	Avpath	Deg	ECC	NNdeg
t	<i>Tsay</i> (1989) <i>Test</i>	0.00***	0.00***	0.01**	0.00***	0.02**
	<i>Tsay</i> (1996) <i>Test</i>	0.01**	0.02**	0.04**	0.03**	0.08*
	<i>Hansen</i> (1996) <i>Test</i>	0.00***	0.00***	0.00***	0.00***	0.04**

Note: Values in this Table denote p-values of linearity tests.

(***), (**), and (*) denote significance at the 1%, 5%, and 10% levels, respectively.

ity is significantly rejected for all network indicators, suggesting that Model 6 is *a priori* not appropriate to model the effect of fragmentation. Furthermore, the rejection of linearity is always significant against abrupt threshold models, suggesting that the data dynamics are characterized by nonlinearity and abrupt threshold effects. Accordingly, we focus next on modeling the relationship between fragmentation and connectivity in a nonlinear framework using a two regime abrupt threshold panel regression.

3.3.4 Panel Threshold Regression Model

We consider Model (7) for which all coefficients are being time-varying across regimes and which extends Model (6) to a nonlinear framework; and we estimate a more general nonlinear model to capture further time variation, asymmetry, and multiple regimes in the data. We report the main results in Table 6.

From Table 6, we note that the assumption of switching regime is not rejected and the transition is appropriately carried out when the transition variable corresponding to fragmentation exceeds a given threshold. In what follows, we comment on the results for the network effects of market fragmentation obtained in the two regimes. As regards distances, when considering the average distance to the nearest neighbours (*AvdistNN*), which is a proxy of local distances, fragmentation has a negative and significant effect. This effect is higher in the second regime. When considering the average path (*Avpath*), which is a proxy of global distances, we find similar results as fragmentation has a negative and significant effect, which is increased in the second regime. The effect of fragmentation is higher for *Avpath* than for *AvdistNN*. As for the eccentricity (*ECC*), which represents maximal distances within the network, fragmentation also has a negative impact on distance whatever the regime under consideration. Although this effect is slightly lower in the second regime, in both regimes it is much more pronounced than the effects on the other distance measures.

For connectivity indicators, when considering the degree of the nodes (*deg*), which is a proxy of local connectivity, we note more asymmetry between regimes as for example more than 90% of the observations are in the first regime. Further, while fragmentation has a positive and significant effect in the first regime, the effect switches and becomes negative in the second regime. This behavior switching is particularly relevant and suitably reproduced by our threshold model, while it does escape the linear modeling.

Table 6: **Results of Panel Threshold Regression Estimate of VoV**

$$y_{i,t} = \begin{cases} \alpha_{1i} + \beta_1 frag_{i,t} + \gamma_1 \ln(Volume_{i,t}) + \delta_1 \frac{1}{price_{i,t}} + \varepsilon_{1i,t} & \text{if } S_{i,t} \leq c \\ \alpha_{2i} + \beta_2 frag_{i,t} + \gamma_2 \ln(Volume_{i,t}) + \delta_2 \frac{1}{price_{i,t}} + \varepsilon_{2i,t} & \text{if } S_{i,t} > c \end{cases}$$

Coefficients	AvdistNN	Avpath	Deg	ECC	NNdeg
Regime 1					
β_1	-0.027*** (0.00)	-0.186*** (0.00)	0.121*** (0.00)	-0.328*** (0.00)	0.008 (0.90)
γ_1	-0.033*** (0.00)	-0.194*** (0.00)	-0.041*** (0.00)	-0.295*** (0.00)	0.068*** (0.00)
δ_1	-0.051*** (0.00)	-1.03*** (0.00)	-0.115*** (0.00)	-0.387*** (0.00)	-0.255*** (0.00)
R^2	0.48	0.39	0.39	0.40	0.16
n_1	31893	32097	59395	33500	38115
$S_{i,t}$	$frag_{i,t}$	$frag_{i,t}$	$frag_{i,t}$	$frag_{i,t}$	$frag_{i,t}$
Regime 2					
β_2	-0.038*** (0.00)	-0.195*** (0.00)	-1.09*** (0.00)	-0.296*** (0.00)	0.171*** (0.00)
γ_2	-0.001 (0.57)	-0.006 (0.41)	-0.047 (0.19)	-0.036*** (0.00)	-0.059** (0.01)
δ_2	0.120*** (0.00)	1.47*** (0.00)	26.2*** (0.00)	1.90*** (0.00)	-5.63*** (0.00)
R^2	0.60	0.49	0.55	0.44	0.09
n_2	33263	33149	5851	31746	27131

Note: R^2 denotes the R-squared. n_1 and n_2 denote the number of observations in regimes 1 and 2 respectively. (***), (**), and (*) denote significance at the 1%, 5%, and 10% levels, respectively. Values in () are the p-values of estimators with White cross-section standard errors & covariance.

Finally, for the nearest neighbours degree ($NNdeg$), which is a proxy of extended connectivity, the effect of fragmentation is not significant in the first regime but positive and statistically significant in the second regime. Otherwise, both control variables behave differently across regimes and show a significant effect on distance and connectivity indicators. This time-variation of control variables effects is also inline with our on-off modeling for the fragmentation effect.

Overall, the effect on connectivity measures is complex and time-varying, whereas this is less the case for distance measures. This result is not as paradoxical as it may seem at first sight. Distance measures describe the size of the network, which generally evolves according to a trend: here it becomes denser, distances are reduced. Connectivity measures, on the other hand, describe the structure of the network, which changes when the network pattern evolves, in particular, with the change of the relative share of linear and star-shaped parts.

In summary, fragmentation decreases individual contributions to the VoV as it decreases all distance measures in both regimes, and this effect increases after the break for local and global measures. Both before and after the break it is the lowest on local distances, stronger on global measures and maximal for the eccentricity. This observation is consistent with the observation of a positive effect of fragmentation on direct connectivity in the first regime (which is the main part of the study period for this variable), and on indirect connectivity in the second regime, which are also in the sense of reduced individual contributions to the VoV. Indeed, the increase in connectivity measures reflects the relative reduction of the linear parts of the network compared to the star pattern parts, which reduces the length of the chains and thus global and maximal distances.

The strong negative effect of fragmentation on direct connectivity in the very short period of time of the second regime is partly explained by the multipolarisation of the network at the end of the study period (see Figure 5). It may also be driven by the very strong decrease of the connectivity of a specific node, Total (FP, see figures 4 and 5). The decrease in the common component of this asset, which is an oil major, is the result of the very sharp drop in oil prices in 2014¹⁰. Although events specific to individual assets generally do not significantly affect network structures, which mainly reflect sectoral affiliations, the case of Total is special for two reasons. First, the firm's profitability is directly linked to the world price of a highly volatile commodity. Second, the asset is originally characterized by a high connectivity. Any specific event affecting its volatility therefore affects its connectivity and, by repercussion, that of the network.

4 Conclusion

We extend the microstructure literature on the effect of trades fragmentation on price formation, and more specially VoV, by combining two major fields of computational

¹⁰For a detailed discussion of the causes and magnitude of the decline in returns on energy portfolios and single-energy investments at the end of 2014, see for example Zhang and Chen (2018).

finance: networks, and non-linear time series. To take the network dimension into account, we rely on the stock market networks literature on minimal spanning trees of price time series. To take the possibility of non-linear financial dynamics into account in the empirical modelling approach, we use threshold models in which all coefficients are time-varying accross regimes. We show that fragmentation affects not only individual volatilities, but also the different network proxies of VoV, and thus its network structure.

In the early regimes, which are globally those of a rapid increase in fragmentation and the adaptation of market operators to the regulatory shock, fragmentation is associated with a decrease in distance measures and a shortening of the linear branches of volatility networks (large decrease in eccentricity, increase in local connectivity). In the latest regimes of fragmentation, where market participants have adapted their trades to the existence of multiple venues, this effect is reinforced and is associated with the increase in extended connectivity. Interestingly, these findings suggest a permanent effect of fragmentation resulting in an increasing density of both the core and the periphery of the network. All network proxies of VoV are affected, and this result is robust to both the specifications tested at the portfolio level and at the individual asset level. This effect is not only nonlinear, as different regimes are associated with the different stages of the dynamics of trades fragmentation; but also heterogeneous, as fragmentation tends to diverge over time.

These results are relevant for several reasons. First, they show that competition between venues has a significant effect on the structure of equity market networks of volatility, which is consistent with the dominant result in the microstructure literature of an effect of market fragmentation on price formation. Second, they show that the effect of fragmentation on the structure of volatility networks is not limited to the learning period when market operators are adapting to a changing regulatory environment. On the contrary, the nonlinear specification shows that this effect can be reinforced in the latest regime. Finally, the application of network indicators enables us to specify the nature of the effect: the whole network is becoming more and more dense, in particular by the convergence of the most remote nodes, with a simultaneous tendency towards a dominant star pattern. To the extent that these indicators are proxies for VoV, our results point to the fact that fragmentation can have significant effects not only on the efficiency of the price formation process; but also on asset returns themselves. From the point of view of investors holding highly fragmented stocks, as well as from the point of view of public authorities and regulators who decide, implement and supervise competition between venues with the objective of improving market efficiency, these results are highly relevant.

References

Bai, J., Perron, P., 2003. Computation and analysis of multiple structural change models. *Journal of applied econometrics* 18, 1–22.

- Baldauf, M., Mollner, J., 2021. Trading in fragmented markets. *Journal of Financial and Quantitative Analysis* 56, 93–121.
- Baltagi, B.H., Feng, Q., Kao, C., 2012. A lagrange multiplier test for cross-sectional dependence in a fixed effects panel data model. *Journal of Econometrics* 170, 164–177.
- Bastidon, C., Parent, A., Jensen, P., Abry, P., Borgnat, P., 2020. Graph-based era segmentation of international financial integration. *Physica A: Statistical Mechanics and its Applications* 539, 122877. URL: <http://www.sciencedirect.com/science/article/pii/S0378437119316346>, doi:<https://doi.org/10.1016/j.physa.2019.122877>.
- Bollerslev, T., Tauchen, G., Zhou, H., 2009. Expected stock returns and variance risk premia. *The Review of Financial Studies* 22, 4463–4492.
- Bonanno, G., Lillo, F., Mantegna, R.N., 2001. High-frequency cross-correlation in a set of stocks. *Quantitative Finance* .
- Bourghelle, D., Jawadi, F., Rozin, P., 2022. Do collective emotions drive bitcoin volatility? a triple-regime switching vector approach. *Journal of Economic Behavior and Organization* , forthcoming.
- Breusch, T.S., Pagan, A.R., 1980. The lagrange multiplier test and its applications to model specification in econometrics. *The review of economic studies* 47, 239–253.
- Brogaard, J., Hendershott, T., Riordan, R., 2014. High-frequency trading and price discovery. *Review of Financial Studies* 27, 2267–2306.
- Brogaard, J., et al., 2010. High frequency trading and its impact on market quality. Northwestern University Kellogg School of Management Working Paper 66.
- Capponi, A., Chen, P.C., 2015. Systemic risk mitigation in financial networks. *Journal of Economic Dynamics and Control* 58, 152–166.
- CBOE, 2022a. Cboe europe market share. URL: http://markets.cboe.com/europe/equities/market_share/.
- CBOE, 2022b. Cboe u.s. equities exchanges overview. URL: http://markets.cboe.com/us/equities/market_statistics/.
- Chaboud, A.P., Chiquoine, B., Hjalmarsson, E., Vega, C., 2014. Rise of the machines: Algorithmic trading in the foreign exchange market. *The Journal of Finance* 69, 2045–2084.
- Chan, J.C., Santi, C., 2021. Speculative bubbles in present-value models: A bayesian markov-switching state space approach. *Journal of Economic Dynamics and Control* 127, 104101.

- Chen, D., Duffie, D., 2020. Market fragmentation. Technical Report. National Bureau of Economic Research.
- Chen, T.F., Chordia, T., Chung, S.L., Lin, J.C., 2022. Volatility-of-volatility risk in asset pricing. *The Review of Asset Pricing Studies* 12, 289–335.
- Chinazzi, M., Fagiolo, G., Reyes, J.A., Schiavo, S., 2013. Post-mortem examination of the international financial network. *Journal of Economic Dynamics and Control* 37, 1692–1713.
- Chlistalla, M., Lutat, M., 2011. Competition in securities markets: the impact on liquidity. *Financial Markets and Portfolio Management* 25, 149–172.
- Cimon, D.A., 2021. Broker routing decisions in limit order markets. *Journal of Financial Markets* 54, 100602.
- Cont, R., 2007. Volatility clustering in financial markets: empirical facts and agent-based models, in: *Long memory in economics*. Springer, pp. 289–309.
- Easley, D., Kiefer, N.M., O'HARA, M., 1996. Cream-Skimming or Profit-Sharing? The Curious Role of Purchased Order Flow. *The Journal of Finance* 51, 811–833.
- Euronext, 2021. Cac 40 index composition and index documents. URL: <https://live.euronext.com/en/product/indices/FR0003500008-XPAR/market-information>.
- Foucault, T., Menkveld, A.J., 2008. Competition for order flow and smart order routing systems. *The Journal of Finance* 63, 119–158.
- Goldstein, M.A., Shkilko, A.V., Van Ness, B.F., Van Ness, R.A., 2008. Competition in the market for nasdaq securities. *Journal of Financial Markets* 11, 113–143.
- Granger, C.W., Terasvirta, T., et al., 1993. *Modelling non-linear economic relationships*. Oxford university press.
- Greenwood-Nimmo, M., Huang, J., Nguyen, V.H., 2019. Financial sector bailouts, sovereign bailouts, and the transfer of credit risk. *Journal of Financial Markets* 42, 121–142.
- Gresse, C., 2017. Effects of lit and dark market fragmentation on liquidity. *Journal of Financial Markets* 35, 1–20.
- Hamilton, J.L., 1979. Marketplace fragmentation, competition, and the efficiency of the stock exchange. *The Journal of Finance* 34, 171–187.
- Hansen, B.E., 1996. Inference when a nuisance parameter is not identified under the null hypothesis. *Econometrica: Journal of the econometric society* , 413–430.

- He, P.W., Jarnećić, E., Liu, Y., 2015. The determinants of alternative trading venue market share: Global evidence from the introduction of chi-x. *Journal of Financial Markets* 22, 27–49.
- Held, M., Karp, R.M., 1970. The traveling-salesman problem and minimum spanning trees. *Operations Research* 18, 1138–1162.
- Horst, E.T., Rodriguez, A., Gzyl, H., Molina, G., 2012. Stochastic volatility models including open, close, high and low prices. *Quantitative Finance* 12, 199–212.
- Iori, G., Mantegna, R.N., 2018. Empirical analyses of networks in finance, in: *Handbook of Computational Economics*. Elsevier. volume 4, pp. 637–685.
- Jawadi, F., Namouri, H., Ftiti, Z., 2018. An analysis of the effect of investor sentiment in a heterogeneous switching transition model for g7 stock markets. *Journal of Economic Dynamics and Control* 91, 469–484.
- Keenan, D.M., 1985. A tukey nonadditivity-type test for time series nonlinearity. *Biometrika* 72, 39–44.
- Kirilenko, A.A., Kyle, A.S., Samadi, M., Tuzun, T., 2014. The flash crash: The impact of high frequency trading on an electronic market. Available at SSRN 1686004 .
- Kruskal, J.B., 1956. On the shortest spanning subtree of a graph and the traveling salesman problem. *Proceedings of the American Mathematical society* 7, 48–50.
- Lim, K., Tong, H., 1980. Threshold autoregressions, limit cycles, and data. *Journal of the Royal Statistical Society, B* 42, 245–92.
- Magdon-Ismail, M., Atiya, A.F., 2003. A maximum likelihood approach to volatility estimation for a brownian motion using high, low and close price data. *Quantitative Finance* 3, 376.
- Mandelbrot, B.B., 2013. *Fractals and scaling in finance: Discontinuity, concentration, risk*. Selecta volume E. Springer Science & Business Media.
- Mantegna, R.N., 1999. Hierarchical structure in financial markets. *The European Physical Journal B-Condensed Matter and Complex Systems* 11, 193–197.
- May, R.M., Levin, S.A., Sugihara, G., 2008. Complex systems: Ecology for bankers. *Nature* 451, 893–895.
- Newman, M.E., 2003. The structure and function of complex networks. *SIAM review* 45, 167–256.
- O’Hara, M., Ye, M., 2011. Is market fragmentation harming market quality? *Journal of Financial Economics* 100, 459–474.

- Pesaran, M.H., 2004. General diagnostic tests for cross-sectional dependence in panels. *Empirical Economics* , 1–38.
- Petrucelli, J., Davies, N., 1986. A portmanteau test for self-exciting threshold autoregressive-type nonlinearity in time series. *Biometrika* 73, 687–694.
- Phillips, P.C., Perron, P., 1988. Testing for a unit root in time series regression. *Biometrika* 75, 335–346.
- Prim, R.C., 1957. Shortest connection networks and some generalizations. *The Bell System Technical Journal* 36, 1389–1401.
- Russell, F., 2021. Industry Classification Benchmark (Equity): Ground Rules. URL: https://research.ftserussell.com/products/downloads/ICB_Rules_new.pdf?_ga=2.123599944.2136867702.1571244687-690700013.1571244687.
- Soramäki, K., Bech, M.L., Arnold, J., Glass, R.J., Beyeler, W.E., 2007. The topology of interbank payment flows. *Physica A: Statistical Mechanics and its Applications* 379, 317–333.
- de Souza, S.R.S., Silva, T.C., Tabak, B.M., Guerra, S.M., 2016. Evaluating systemic risk using bank default probabilities in financial networks. *Journal of Economic Dynamics and Control* 66, 54–75.
- Terasvirta, Timo andc, D., Granger, C.W., et al., 2010. *Modelling nonlinear economic time series*. Oxford University Press.
- Tong, H., 1990. *Non-linear time series: a dynamical system approach*. Oxford University Press.
- Tong, H., Lim, K., 1980. Threshold autoregression, limit cycles and cyclical data. *Journal of the Royal Statistical Society. Series B (Methodological)* , 245–292.
- Tong, H., Lim, K.S., 2009. Threshold autoregression, limit cycles and cyclical data, in: *Exploration Of A Nonlinear World: An Appreciation of Howell Tong’s Contributions to Statistics*. World Scientific, pp. 9–56.
- Tsay, R.S., 1986. Nonlinearity tests for time series. *Biometrika* 73, 461–466.
- Tsay, R.S., 1989. Testing and modeling threshold autoregressive processes. *Journal of the American statistical association* 84, 231–240.
- Tsay, R.S., 1998. Testing and modeling multivariate threshold models. *journal of the american statistical association* 93, 1188–1202.
- Tumminello, M., Coronello, C., Lillo, F., Micciche, S., Mantegna, R.N., 2007. Spanning trees and bootstrap reliability estimation in correlation-based networks. *International Journal of Bifurcation and Chaos* 17, 2319–2329.

- Yang, D., Zhang, Q., 2000. Drift-independent volatility estimation based on high, low, open, and close prices. *The Journal of Business* 73, 477–492.
- Zhang, F., 2010. m. Available at SSRN 1691679 .
- Zhang, T., 2021. Stock prices and the risk-free rate: An internal rationality approach. *Journal of Economic Dynamics and Control* 127, 104103.
- Zhang, Y.J., Chen, M.Y., 2018. Evaluating the dynamic performance of energy portfolios: Empirical evidence from the dea directional distance function. *European Journal of Operational Research* 269, 64–78.

Appendix

Table I: Descriptive Statistics: Time Series of Market Fragmentation

	Mean	Median	Stdev	Min	Max	Skew	Kurt	Percent5	Percent95
CAC 40	1,918	1,993	0,267	1,103	2,268	-1,290	4,087	1,315	2,200
ACCOR	1,954	1,999	0,345	1,050	2,980	-0,410	3,149	1,301	2,442
AIR LIQUIDE	1,812	1,847	0,238	1,047	2,310	-1,086	4,494	1,261	2,122
AIRBUS GROUP	1,917	1,948	0,342	1,081	2,815	-0,388	2,719	1,290	2,403
ALCATEL-LUCENT	1,901	1,987	0,410	1,121	2,669	-0,270	1,823	1,230	2,469
ALSTOM	1,909	1,970	0,289	1,050	2,745	-0,954	4,060	1,276	2,262
AXA	1,910	1,956	0,296	1,179	2,494	-0,590	2,775	1,307	2,327
BNP PARIBAS ACT.A	1,880	1,951	0,296	1,119	2,495	-0,910	3,145	1,247	2,254
BOUYGUES	1,869	1,872	0,278	1,087	2,584	-0,468	3,089	1,328	2,283
CAP GEMINI	1,904	1,934	0,316	1,094	2,637	-0,383	2,711	1,314	2,352
CARREFOUR	1,807	1,849	0,244	1,074	2,271	-0,998	4,005	1,233	2,136
CREDIT AGRICOLE	1,981	2,071	0,349	1,107	2,639	-0,694	2,671	1,289	2,432
DANONE	1,954	2,006	0,282	1,081	2,512	-1,053	4,210	1,323	2,329
DEXIA	1,347	1,303	0,269	1,000	2,578	1,343	5,253	1,037	1,842
EDF	1,852	1,857	0,294	1,045	2,494	-0,472	3,438	1,289	2,311
ESSILOR INTL.	1,899	1,924	0,312	1,048	2,591	-0,661	3,305	1,308	2,357
GDF SUEZ	1,863	1,912	0,294	1,026	2,481	-0,912	3,620	1,175	2,265
KERING	1,920	1,957	0,321	1,062	2,480	-0,761	3,178	1,269	2,356
LAFARGE	1,848	1,891	0,289	1,061	2,513	-0,697	3,284	1,241	2,244
LAGARDERE S.C.A.	1,916	1,863	0,379	1,047	3,231	0,181	3,017	1,268	2,563
L'OREAL	1,875	1,926	0,267	1,050	2,367	-1,203	4,317	1,254	2,202
LVMH	1,938	1,988	0,299	1,076	2,541	-0,832	3,436	1,289	2,335
MICHELIN	1,981	2,048	0,304	1,052	2,548	-1,124	4,070	1,329	2,356
ORANGE	1,909	1,954	0,267	1,101	2,403	-1,163	4,192	1,285	2,248
PERNOD RICARD	2,016	2,069	0,343	1,063	2,726	-0,871	3,363	1,281	2,450
PEUGEOT	1,953	1,995	0,368	1,069	2,787	-0,309	2,389	1,312	2,478
RENAULT	2,008	2,093	0,371	1,060	2,629	-0,598	2,511	1,295	2,501
SAINT GOBAIN	1,890	1,900	0,292	1,071	2,641	-0,594	3,511	1,271	2,326
SANOFI	1,947	2,009	0,293	1,070	2,536	-1,079	3,838	1,293	2,302
SCHNEIDER ELECTRIC	1,968	2,003	0,280	1,072	2,603	-1,026	4,500	1,346	2,358
SOCIETE GENERALE	1,844	1,925	0,276	1,098	2,346	-0,998	3,317	1,237	2,171
STMICROELECTRONICS	2,047	2,010	0,429	1,099	3,154	0,148	2,541	1,344	2,783
SUEZ ENVIRONNEMENT	1,912	1,909	0,342	1,000	2,763	-0,422	3,346	1,251	2,428
TECHNIP	1,908	1,922	0,412	1,000	2,839	-0,468	2,943	1,001	2,524
TOTAL	1,961	1,979	0,265	1,156	2,728	-0,455	4,422	1,403	2,395
UNIBAIL-RODAMCO	1,777	1,834	0,285	1,059	2,381	-0,669	2,895	1,189	2,156
VALLOUREC	1,897	1,926	0,336	1,048	2,637	-0,357	2,938	1,276	2,445
VEOLIA ENVIRON.	1,876	1,894	0,291	1,045	2,666	-0,618	3,442	1,282	2,291
VINCI	1,850	1,891	0,273	1,061	2,554	-0,717	3,599	1,266	2,245
VIVENDI	1,899	1,933	0,264	1,073	2,514	-0,934	4,012	1,325	2,251

Source: Fidessa.

Table II: ICB Sectors of the Assets of the Sample

ICB sector		Ticker	
Alcatel	1 Technology & Telecom.	10 Technology	ALU
CapGemini		10 Technology	CAP
STMicroelectronics		10 Technology	STM
Orange	2 HealthCare	15 Telecommunications	ORA
Essilor		20 HealthCare	EL
SanofiSynthelabo		20 HealthCare	SAN
BNP	3 Financials & Real estate	3010 Banks	BNP
Credit Agricole		3010 Banks	ACA
Dexia		3010 Banks	DEXB
SocieteGenerale		3010 Banks	GLE
Axa		3030 Insurance	CS
UnibailRodamco	4 Consumer discretionary & Staples	35 Real Estate	URW
Michelin		4010 Automobiles&Parts	ML
Peugeot		4010 Automobiles&Parts	UG
Renault		4010 Automobiles&Parts	RNO
Lagardere		4030 Media	MMB
VivendiUniversal		4030 Media	VIV
Carrefour		4040 Retailers	CA
KeringPPR		4040 Retailers	KER
Accor		4050 Travel&Leisure	AC
Danone		4510 Food Beverage&Tobacco	BN
PernodRicard		4510 Food Beverage&Tobacco	RI
LOreal		4520 Personal Care,Drug&Grocery Stores	OR
LVMH		4520 Personal Care,Drug&Grocery Stores	MC
Bouygues	5 Indus. & Basic mat.	5010 Construction&Materials	EN
Lafarge		5010 Construction&Materials	LHN
SaintGobain		5010 Construction&Materials	SGO
Vinci		5010 Construction&Materials	DG
AirbusEADS		5020 Industrial Goods&Services	AIR
Alstom		5020 Industrial Goods&Services	ALO
Schneider		5020 Industrial Goods&Services	SU
Vallourec		5020 Industrial Goods&Services	VK
ArcelorMittal		5510 Basic Ressources	MT
AirLiquide		5520 Chemicals	AI
Technip	6 Energy & Utilities	601010 Oil Gas&Coal	FTI
Total		601010 Oil Gas&Coal	FP
EDF		65 Utilities	EDF
GDFSuez		65 Utilities	ENGI
Suez		65 Utilities	SEV
VeoliaEnvironnement		65 Utilities	VIE

Source: Euronext (2021) and Russell (2021). The CAC40 factsheet classification is composed of 18 categories, among which 2 digits codes correspond to Industries, 4 digits to Supersectors and 6 digits to Sectors in the ICB classification.

Table III: **Descriptive Statistics: Time Series of Volatilities**

	Mean	Median	Stdev	Min	Max	Skew	Kurt	Percent5	Percent95
Accor	0,027	0,023	0,016	0,002	0,217	2,279	14,391	0,010	0,058
AirLiquide	0,032	0,026	0,021	0,001	0,280	2,765	19,170	0,012	0,069
AirbusEADS	0,022	0,018	0,015	0,041	0,504	9,726	276,404	0,009	0,046
Alcatel	0,042	0,034	0,027	0,002	0,267	2,312	12,335	0,015	0,092
Alstom	0,041	0,031	0,038	0,004	0,853	5,521	72,540	0,012	0,101
ArcelorMittal	0,032	0,027	0,020	0,004	0,216	2,589	13,333	0,012	0,069
Axa	0,033	0,026	0,023	0,006	0,239	2,467	12,131	0,012	0,079
BNP	0,030	0,024	0,021	0,002	0,211	2,580	13,178	0,011	0,073
Bouygues	0,029	0,024	0,018	0,005	0,168	2,024	9,342	0,010	0,064
CapGemini	0,033	0,027	0,022	0,002	0,268	2,286	12,515	0,011	0,074
Carrefour	0,026	0,022	0,015	0,003	0,142	1,931	8,885	0,010	0,054
CreditAgricole	0,033	0,026	0,022	0,001	0,259	2,198	11,589	0,011	0,077
Danone	0,021	0,018	0,012	0,003	0,135	2,469	14,065	0,009	0,044
Dexia	0,034	0,025	0,034	0,001	0,483	4,546	39,287	0,008	0,093
EDF	0,024	0,021	0,014	0,004	0,162	2,355	12,676	0,010	0,050
Essilor	0,021	0,018	0,013	0,004	0,176	2,617	16,913	0,009	0,046
GDFSuez	0,027	0,022	0,018	0,002	0,227	3,139	19,593	0,011	0,061
KeringPPR	0,026	0,021	0,018	0,002	0,184	2,401	12,253	0,009	0,061
LOreal	0,028	0,023	0,018	0,002	0,196	2,440	13,227	0,010	0,061
Lafarge	0,028	0,023	0,018	0,001	0,193	2,408	12,874	0,010	0,061
Lagardere	0,023	0,020	0,014	0,005	0,132	2,025	9,423	0,009	0,050
IVMH	0,026	0,022	0,016	0,005	0,163	2,227	11,305	0,010	0,058
Michelin	0,029	0,025	0,017	0,002	0,169	2,117	10,482	0,011	0,061
Orange	0,029	0,022	0,022	0,002	0,230	2,655	13,630	0,010	0,070
PernodRicard	0,022	0,018	0,014	0,003	0,157	2,561	13,385	0,009	0,049
Peugeot	0,033	0,029	0,019	0,001	0,207	1,824	8,736	0,012	0,070
Renault	0,033	0,028	0,019	0,004	0,175	2,052	9,832	0,012	0,069
SaintGobain	0,030	0,025	0,019	0,000	0,376	3,324	36,114	0,011	0,065
SanofiSynthelabo	0,025	0,021	0,015	0,002	0,145	2,016	9,258	0,010	0,053
Schneider	0,028	0,024	0,017	0,005	0,182	2,177	11,726	0,010	0,060
SocieteGenerale	0,034	0,029	0,024	0,004	0,331	2,835	18,966	0,011	0,081
STMicronelronics	0,033	0,027	0,019	0,001	0,202	2,054	10,195	0,012	0,069
SuezLyonnaise des eaux	0,025	0,021	0,015	0,004	0,146	2,386	12,688	0,010	0,054
Technip	0,031	0,026	0,020	0,005	0,226	2,840	17,986	0,011	0,066
Total	0,022	0,019	0,012	0,004	0,111	1,997	9,111	0,009	0,045
UnibailRodamco	0,022	0,019	0,013	0,001	0,101	1,797	7,772	0,008	0,047
Vallourec	0,031	0,026	0,019	0,002	0,210	2,066	9,991	0,011	0,068
VeoliaEnvironnement	0,028	0,023	0,019	0,004	0,275	3,041	20,255	0,011	0,062
Vinci	0,024	0,021	0,015	0,004	0,177	2,450	14,038	0,009	0,051
VivendiUniversal	0,029	0,022	0,026	0,001	0,420	4,955	47,197	0,010	0,072

Table IV: **Descriptive Statistics: Time series of topological Indicators**

	Mean	Median	Stdev	Min	Max	Skew	Kurt	Percent5	Percent95
Av. path	2,732	2,739	0,784	0,685	5,285	0,042	2,867	1,433	4,023
Eccentricity	6,255	6,194	1,912	1,703	13,337	0,234	3,045	3,137	9,496
Degree	1,488	1,469	0,220	0,899	2,350	0,401	2,978	1,154	1,888
Av. NN dist.	0,675	0,693	0,130	0,203	0,897	-0,889	3,632	0,429	0,848
NN degree	3,452	3,353	0,543	2,344	6,087	1,005	4,333	2,748	4,492